Acoustic Emission Analysis of Fatigue Failure of LMFBR Primary Coolant Piping

January, 1975

POWER REACTOR AND NUCLEAR FUEL DEVELOPMENT CORPORATION

〒319-1184　茨城県那珂郡東海村大字村松4番地49
核燃料サイクル開発機構
技術展開部　技術協力課

Inquiries about copyright and reproduction should be addressed to:
Technical Cooperation Section,
Technology Management Division,
Japan Nuclear Cycle Development Institute
4-49 Muramatsu, Tokai-mura, Naka-gun, Ibaraki, 319-1184
Japan

TN251 75-01
Jan., 1975

Acoustic Emission Analysis on Fatigue Failure of LMFBR Primary Coolant Piping*

Hironori Ono**
Hiroyasu Nakasa**
Tadao Machida**
Yoshio Tomoda**
Mitsuo Fukushima**
Kiyoshi Takigawa**
Masao Hori,
Kunio Okabayashi,
Shuzo Ueda,
Takashi Nagata, and
Masayuki Kikuchi.

Abstract

Recently, "acoustic emission (AE) analysis" calls attention as a dynamic and non-destructive material testing method. We can get information of material defects and cracks by catching acoustic signals from themselves, so it may be possible to know the propagation of latent cracks dynamically, to find the location of defects or to predict the failure. Therefore it may be said that this "acoustic emission method" is one of the best methods of the inservice inspection of the primary coolant piping of liquid metal cooled fast breeder reactor (LMFBR).

But for the application of this method, in addition to the fundamental tests, it is necessary to recognize AE characteristics of the piping by the experimental measurement of the AE signals in the cyclic loading test of the piping components. For this purpose, a contract of cooperative work was made between CRIEPI who had much experience in AE measurement in the material tests and PNC

This is the translation of the report, No. J256 73-02, issued in Jan., 1973.

* Work performed by Central Research Institute of Electric Power Industry (CRIEPI) under contract with Power Reactor and Nuclear Fuel Development Corp.

** CRIEPI.

who was doing cyclic fatigue test of the piping components. There it was agreed that in close cooperation the development of instrumentation system, the analysis of measured AE data and the operation and the analysis of the piping component model fatigue tests should be done.

In the acoustic emission signals from the material, there are two types; one is the continuous AE signal accompanied by the plastic deformation of the material, and the other is the burst type AE signal accompanied by cracking. The experimental test was purposed to gain data of these AE signals in the fatigue test.

The AE signals have three fundamental characteristics; frequency, amplitude and emission rate. As for frequency, the investigation focused both on 100 kHz signal which was thought to be the representative frequency of the continuous type and on 1 MHz signal which was thought to be the representative frequency of the burst type. Amplitude and emission rate were monitored by transforming AE signals through the preamplifier and the main amplifier, to analog outputs with an AM converter and a pulse converter, and outputs were recorded with the pen recorders, digital counters, tape recorder, etc. Analyses were done on the variation of the amplitude, the emission rate and the amplitude-emission rate relationship with cycles, and were done on the total counts through cycles in the later high temperature test.

For the transducer of the AE probe, we used PZT ceramics, which has a large dielectric constant, and a high Curie point. Probes were fixed on the piping model by a binding band or by a wave guide bar.

In the early tests of bend-type models, it was confirmed that the acoustic emission rate clearly increased in the stage of crack propagation, especially near the stage in which cracks propagate finally through thickness. But in the tests of the branch-type model, AE characteristics could not be obtained clearly because 20 mmϕ probes which were of low sentivity were used.

In the high-temperature (550 $^{\circ}$C) test, in addition to those measured in the proceeding tests, total AE counts were measured by a counter. Amplitude and emission rate of the AE signals were both greater than those in the room-temperature tests of the same

type model. Furthermore, it was thought that the cycles of initiation and those of through-thickness propagation of fatigue cracks could be estimated from the trend of the curve of the total counts.

As for AE amplitude-emission rate relationship, tangent in the log-log plot has a tendency of decrease in the presence of cracks.

In conclusion, acoustic emission instrumentation systems developed in this research were operated successively in the final stage of experiments. Preliminary and important data with regard to the inspection of fatigue damage of piping models were obtained at room and high temperatures.

--- CONTENTS ---

1. Preface

Since 1971, the FBR Safety Laboratory of Power Reactor and Nuclear Fuel Development Corporation (PNC) has undertaken a fatigue test of stainless steel piping of thin wall under room and high temperatures taking FBR piping components as a model, and now is continuing subsequent tests for the purpose of evaluating the method and technique for calculation of the fatigue life of the piping components.

In these fatigue tests of piping components, a preliminary study was made by the concerned people in PNC and the Central Research Institute of Electric Power Industry (CRIEPI) to utilize the so-called "Acoustic Emission Analysis" or "Stress Wave Emission Analysis," which was drawing a mounting attention of the concerned quarters as a unique method for dynamic and non-destructive tests of materials, as the means to detect and determine the initiation of fatigue crack and the process of its propagation. As the outcome of a series of meetings held on this subject since January 1972, PNC and CRIEPI have agreed to undertake a joint research and experimental work on the following basis:

(1) Subject: Analysis and follow-up of the process of fatigue failure of LMFBR primary sodium coolant loop piping by use of the Acoustic Emission Analysis Method.

(2) Object: Feasibility assessment of the follow-up of the process of fatigue failure including the initiation of a crack and its propagation on the primary coolant circuit piping of LMFBR by means of the Acoustic Emission Analysis, and a preliminary study and

research of this method for its practical use in the future.

(3) Items to be worked on:

i) Acoustic emission monitoring during the fatigue test of the primary coolant loop piping elements.

ii) Analysis of the test results.

iii) Evaluation of feasibility and usefulness of the acoustic emission analysis for the follow-up of the process of fatigue failure of the piping.

iv) Program and allocation of work:

a) Preparation of test specimens by PNC

b) Preparation of acoustic emission circuits by CRIEPI

c) Preparation of fatigue failure monitoring circuits by PNC

d) System operation test on test specimens

e) Data measuring by PNC and CRIEPI

f) Analysis of the acoustic emission data by CRIEPI

g) Analysis of the fatigue failure data by PNC

h) Evaluation of the usefulness of the follow-up technique by means of the acoustic emission method by PNC and CRIEPI

i) Publication of a joint research report by PNC and CRIEPI

(4) Period: March 21, 1972 - December 31, 1973

This report, which has compiled the test data obtained in the

above mentioned joint research work, and the basic research data, which had been acquired as the result of the preliminary research undertaken before the execution of the contract relating to application of the acoustic emission analysis to the fatigue test of the FBR sodium coolant piping components, is an interim report covering mainly the research progress upto October 1972.

Chapter 2 of this report introduces the outline of the acoustic emission analysis based on the basic research conducted by CRIEPI. Chapter 3 covers the results of the acoustic emission analysis which was employed in the tests such as the fatigue tests of bend pipes BE-4 and BE-5 at room temperature which were performed in February this year, and the fatigue tests of branch pipes BR-4 and BR-5 at room temperature performed respectively in March and April this year, and the high temperature test of BR-6 conducted in May and during the months of September and October. The final (Chapter 4) reviews the problems concerning the technique of the acoustic emission analysis and the acoustic emission behavior of the piping components.

2. Outline of Acoustic Emission Analytical Technique

2-1. Acoustic Emission Characteristics of Solid Material

When external forces are applied, not only metals but also other solid materials emit characteristic acoustic waves corresponding to each stage of their physical change during the process of their deformation and final breakdown. Such a sound emission is called "Acoustic Emissions" (abbreviated as AE) or "Stress Wave Emission," and is the focus of attention lately as a helpful method for use in dynamic non-destructive material test and monitoring

As more practical interest preceded, neither causing mechanism of AE nor its characteristic nature have yet been known sufficiently up to the present time. It is, however, known that AE can roughly be classified into two major categories; namely a "continuous type AE" or "small amplitude AE" arising from plastic deformation, and a "burst type AE" or "large amplitude AE". These two types have the following performance features:

(1) Continuous Type AE

a) This is assumed to be originated from such micro-defects as pileup and breakaway of dislocations, twinning, or rotation of crystal orientation. Its energy level is estimated to be at 1 - 10eV.

b) The wave form observed is like a continuous noise because of a large number of emission for a unit of time.

c) This type of AE occurs in the time span from low stress to outset of the plastic deformation, and as deformation advances, the amplitude and the count-rate increase reaching the maximum near the yielding point.

d) AE count is non-reversible to stress. That is, when a material which once was subjected to a load in the past is placed under a load again, it will not produce AE signals until its load exceeds its previously experienced maximum load. That is the so called "Kaiser effect."

(2) Burst Type AE

a) This type of AE is thought to occur from macroscopic defects such as a small crack. Its energy level is estimated to be 10^{10} - 10^{14} times as large as that of the continuous type AE.

b) Its energy level is so large that its amplitude is also large compared with the continuous type AE. But its count-rate is low and its is in the form of a sharp impulse involving waves of frequency.

c) It occurs in the process from the beginning of plastic deformation to the final breakdown. Toward the final stage of breakdown, the count rate shows a drastic increase.

d) Before and after the burst type AE, there takes place the continuous type AE, and because of the changes in the stress distribution accompanied by it, Kaiser effect is not clear in many cases.

e) It has been recognized that the amplitude of AE corresponds to the propagation length of a crack, and that the count-rate corresponds to the propagation speed of the crack. Also, it has been confirmed that the accumulated number of AE is related with the square of the crack length, and that the total sum of the signal amplitude relates with the developed crack length.

In this work, of which the object was to follow-up the fatigue failure process of the FBR primary coolant loop piping components, it was tried to obtain informations about the fatigue crack initiation and its propagation during the fatigue test by observing the phenomenon of the burst type AE and those of the continuous type AE appearing before and after burst type AE, making use of the characteristic behaviors of both continuous and burst types of AE, i.e., the former occurs at the time of dislocation motion where a plastic deformation takes place and the latter is caused by the propagation of a macro-defect. For this purpose, it was necessary to sufficiently grasp the AE performance feathres in the fatigue test. Generally, the basic performance of AE can be characterized by the three quantities - frequency, amplitude, and the count-rate. The frequency characteristics mean the AE wave form or the frequency spectrum which is equivalent to Fourier transform of the wave form, the amplitude feature means to the time change of AE amplitude or to the amplitude distribution per unit of time, and the count-rate characteristics represent the AE counts per unit of time or the cumulative total counts equivalent to the integral of the count rate. These AE performance characteristics are depend upon the mechanical properties of the test materials, presence of micro- and macroscopic defects as well as the mechanism of their initiation and subsequent growth or propagation, and also are influenced by external conditions such as load and temperature.

2-2. Measuring and Analytical Methods of AE

The AE measurement and analysis system generally consists of the following items:

a) Sound Detection System: Acoustic probe pre-main amplifier.

b) Sound Direct Indicating System: (Wave form observation system) Braun tube oscilloscope, Transient recorder, Pen-recorder with detector amplifier.

c) Data Recording System: High speed data recorder, Tape-recorder with a frequency converter.

d) Frequency Discrimination and Analysis System: High-pass and band-pass filter, Frequency spectrum analyzer.

e) Amplitude - Count-Rate Analysis System: Amplitude discriminator, Ratemeter, Counter, Single or multi-channel pulse height analyzer

(1) Sound Detection System: The transducer element which is used for sound probing is generally a voltage type transducer-element to cope with the high frequency of the concerning sound. For such a transducer-element, it is desired that it has a large dielectric constant $\varepsilon / \varepsilon_0$, and voltage output coefficient g, and a high Curie point T_c. Normally, PZT ceramic transducer-element is used. (Refer to Table 2-1.)

This voltage type transducer-element has a resonance frequency fr, and only the signal components within certain band range centering on this frequency can be detected in high sensitivity. The equivalent circuit of the transducer-

Table 2-1. PZT Ceramics

Composition	$Pb(Zr_x Ti_{1-x})O_3$ $x = 0.4 - 0.6$
Density P	7.50 g/cm^3
Dielectric constant $\varepsilon / \varepsilon_o$	1.100
Voltage output coefficient g	32×10^{-3} V·m/N
Frequency constant N = frl	180 KHz - cm
Curie point Tc	360 °C

(Radiation-proof is fairly good)

element in the vicinity of the resonance frequency is as shown by Fig. 2-1.

$$f_r = \frac{1}{2\pi\sqrt{LC}}$$

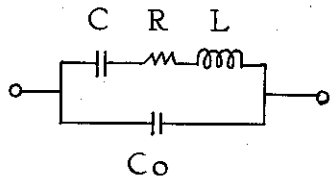

Fig. 2-1

As the product of the resonance frequency f_r and the thickness l of the transducer-element, N = f_rl, is a constant value called "Frequency constant", there arise the "maximum" and the "minimum" with regard to f_r of the transducer-element due to its manufacturing condition (the maximum is about 2 MHz.). Because of this frequency characteristics of the transducer-element, the wave form of AE detection signal is subject to a great influence of the transducer-element. For instance, a sharp impulse type wave form at the source of AE may be deformed into a long, dragging ringing type wave form.

The structure of the probe and the method of its fitting to the test body constitute a big problem in the sound detection system. In many cases, in the measurement of AE, a round shaped transducer-element is employed in order to make it possible to catch AE which may come from any direction. It is therefore desirable that this circular-form transducer-element should have a lining to attenuate the above mentioned linking wave. For the fitting of the probe to the test material, the normally adopted method is that an electrically insulated sound transmitting medium is inserted between the probe and the test material so that no inductive electrical noise will be picked up. In this test, we used sheets of silicon-rubber coated with silicon grease in the earlier tests, while in the latter part of the tests, we tried with sheets of paper coated with silicon grease.

It is also possible to use a high temperature transducer-element for the high temperature acoustic probe. Due to the difficulties in finding effective insulation materials as well as structural materials, the mechanical wave-guides are employed recently, and relatively low temperature acoustic probes are adopted. The Battelle Laboratories is using either a ziralloy or stainless steel rod of 1/8"ϕ with a cup on the side of the test material. Attenuation of 700KHz acoustic wave propagating in this waveguide is said to be 0.2 dB/ft.

As the output impedance of the piezo-electric element is considerably large, the capacity being several tens to several hundres pF, an impedance conversion is performed by use of a pre-amplifier to lower the output impedance. Also,

deterioration of its S/N ratio by electrical inductive noises is prevented by amplifying the signal by about 40 dB.

When electrical inductive noises are too large, it is possible to control them by use of such a type of transducer-element which is capable of producing a balanced output by insulating both poles of the transducer-element and furthermore by use of a differential amplifier for the pre-amplifier, thus surpressing noise arising in the same phase.

(2) Wave Form Observation System

A CRT oscilloscope is used for observation of the wave form of AE signal and a short-time emission rate, while for a prolonged observation and monitoring, a pen-recorder with a detector amplifier is used. The transient recorder is a kind of digital type memoryscope which is capable of recording and accumulating AE signal wave forms and other instantaneous phenomena, and at the same time, these records can be reproduced by CRTs and X-Y recorders.

(3) Data Recording System

In order to analyze AE performance closely, it is desired to check on the measured data repeatedly from various aspects after AE data are recorded. Also, with a frequency conversion, i.e., by an envelop detection (of the amplitude modulation), of the high frequency AE signal wave, it is possible to lower the frequency down to an audible range. The record of the audible signal on an audio-tape recorder is sufficient for the analysis of AE amplitude and the count-rate characteristics. (Refer to Fig. 2-2.)

Fig. 2-2. Signal Processing (1)

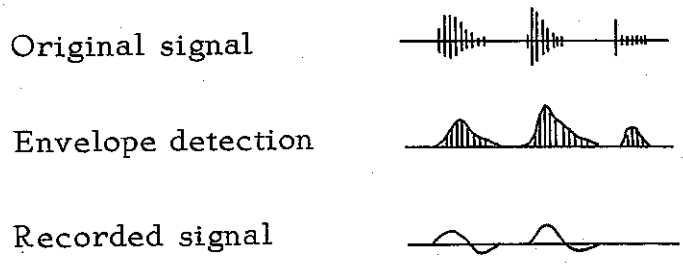

(4) Frequency Discrimination and Analysis System

In order to tentatively catch the frequency characteristics of AE signal and the frequency spectrum of the environmental noises, the correlation of frequency and strength was checked on by use of a frequency spectrum analyzer. After the frequency range which can obtain the optimum S/N ratio of AE signal against the environmental noises is determined, a frequency discrimination is made by use of a transducer-element which has a resonance point in the above mentioned band range, and an HP or BP filter.

(5) Amplitude - Counter-rate Analysis System

For AE monitoring, i.e., to obtain either the cumulative total counts or the count-rate, we use an amplitude discriminator which will emit a certain form of voltage pulses when a signal with an amplitude beyond a certain level is input.

As it is difficult to judge the appropriate choice of amplitude level for pulse emission, it is desirable to have a multi-stage amplitude.

For the detailed analysis of AE amplitude - count-rate characteristics, a multi-channel pulse height analyzer is applied to the recorded AE data. In this case, as shown by

Fig. 2-3, a transducer which emits extremely short time pulses with heights corresponding to the amplitudes of the recorded low frequency signals is employed.

Fig. 2-3. Signal Processing (2)

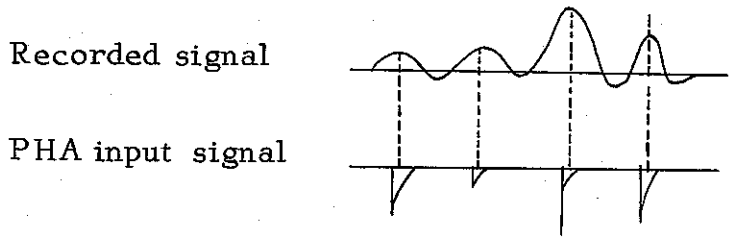

The multi-channel pulse height analyzer is capable of performing the following three modes of AE performance analysis: These analytical data are displayed analogically on an X-Y recorder, or digitally on an electric typewriter.

a) PHA mode: Amplitude - count-rate, or cumulative total counts.

b) Multi-scaler mode: Time - count-rate.

c) Analogic mode: Phase (of load or displacement) - count-rate or total counts.

2-3. AE Characteristics of Stainless Steel Test Pieces Under Tensile Test

Small test pieces of SUS 304 (18-8 stainless steel), which is the piping material of the FBR's primary sodium coolant loop were subjected to a single and repeated tensile tests by an Instrone tensile tester, and the AE characteristics investigated during those tensile tests are given as follows:

Normally, the 18-8 stainless steel has the physical constants as shown in Table 2-2, and under room temperature, it has an

austenitic face centered cubic (fcc) crystal structure. Due to these properties, it is rich in ductility and toughness. For this reason, although its mechanical property can not be changed by heat treatment, its cold processing is not difficult, and it has a physical characteristics of becoming rigid and tough by processing or working.

Table 2-2. Physical Properties of SUS 304 Stainless Steel

Density γ	$7.82 \times 10^3 kg/m^3$
Melting point Tm	1410 °C
Heat conductivity rate λ	14 Kcal/m.hr.°C
Specific heat c	0.118 Kcal/kg.°C
Linear expansion rate β	16.7×10^{-6}/°C
$a = \lambda / cr$	$0.016\ m^2/hr$

Fig. 2-4 - 2-9 show AE measured data of 18-8 stainless steel.

Fig. 2-4. Simple tension of material as received.

Fig. 2-5. Simple tension of material as received and 800 °C x 1hr. annealed material.

Fig. 2-6. Simple tension of 100 °C x 1hr. aged material.

Fig. 2-7. Simple tension of worked material.

Fig. 2-8. Repeated tension of 800 °C x 1hr. annealed material.

Fig. 2-9. Repeated tension of material as received with 2mm notch.

AE characteristics of 18-8 stainless steel are summarized

as follows from the data which were obtained from the above listed tensile tests:

(1) 18-8 stainless steel shows fewer AE signals compared with other materials. In the tensile test of this material as received, AE count-rate increased a little when a crack appeared immediately after tension was applied on it (in the vicinity of the yielding point) as well as when the material broken down.
Refer to Fig. 2-4.

(2) In an annealed material the peak of the AE count-rate rises at initiation of tension. But the AE in the work-hardened area declines. (Refer to Fig. 2-5)

(3) The 100 °C x 1hr. aged material has a high AE count frequency in the work-hardened area. (Refer to Fig. 2-6)

(4) The material 1hr. aged after work at 100 °C has a strong trend of higher frequency of AE counts. (Refer to Fig. 2-7)

(5) From the fatigue test data given in Figures 2-8 and 2-9, the following can be said:

a) In the initial loading of the tensile test, at 100KHz, a Kaiser effect can be recognized, but at 600KHz, no visible Kaiser effect is detected.

b) AE count-rate is large after commencement of the constant cycle, and gradually declines and becomes sporadic. But corresponding to the initiation of a fatigue crack and its propagation, it again increases. This phenomenon can be more clearly indicated when expressed in a form of "Repetition cycles - AE cumulative total counts" as shown in Fig. 2-9, where gradient changes occur following the crack initiation and its propagation.

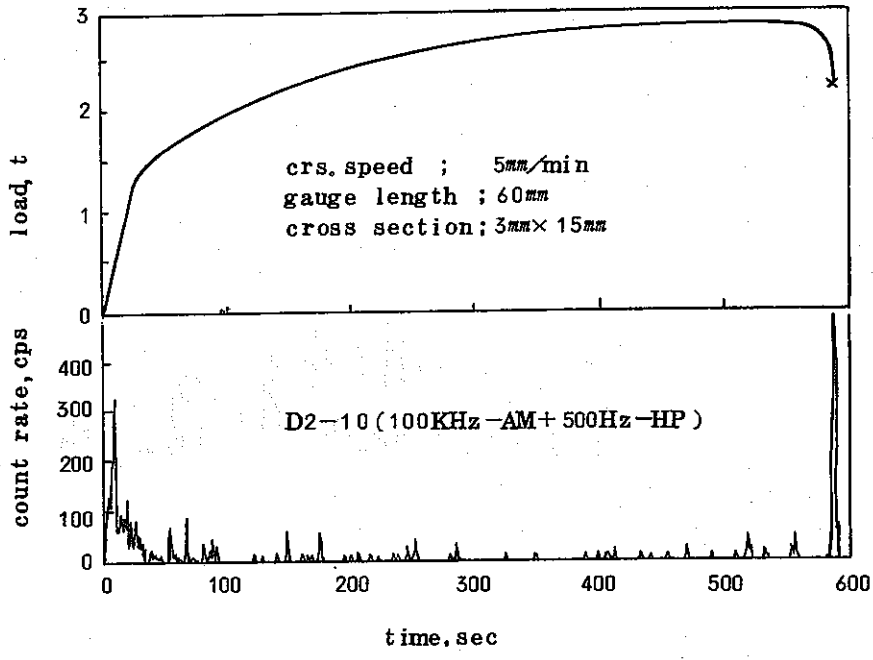

Fig. 2-4. AE of SUS 304 Stainless Steel (As Received) Under Tension

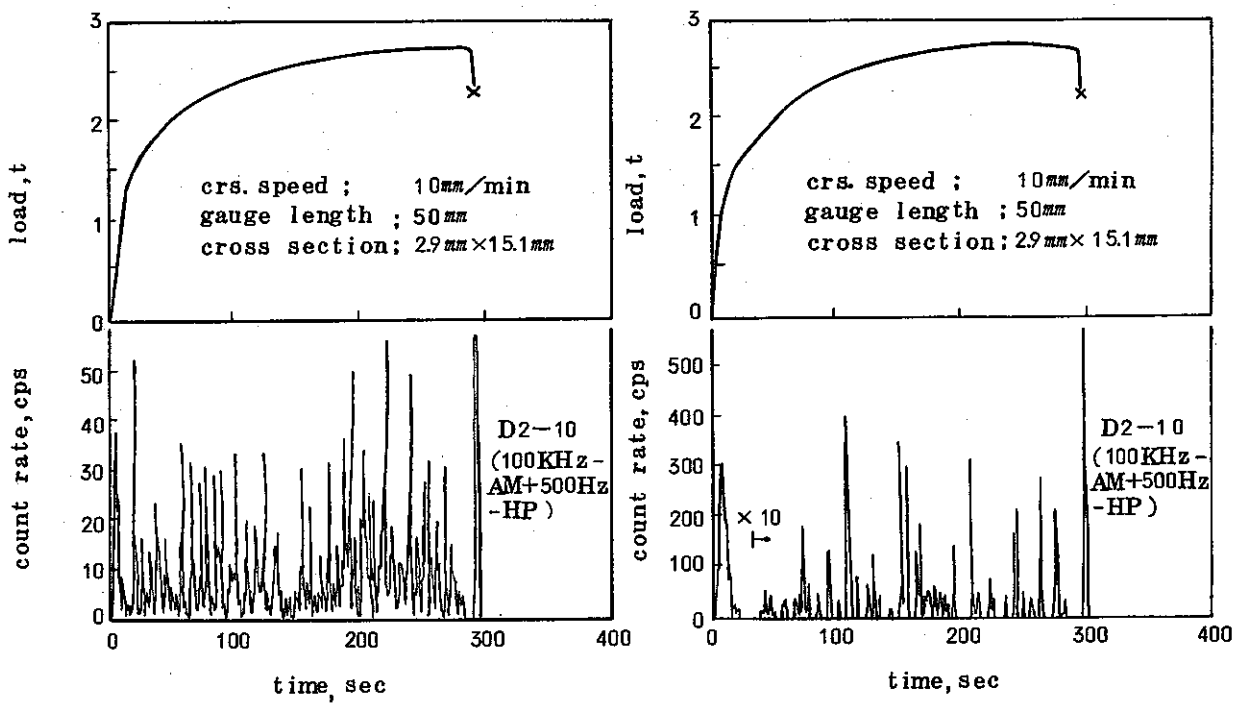

a) as received b) 800℃, 1hr annealed

Fig. 2-5. AE of SUS 304 Stainless Steel Under Tension — Stress Relief Annealing Effect

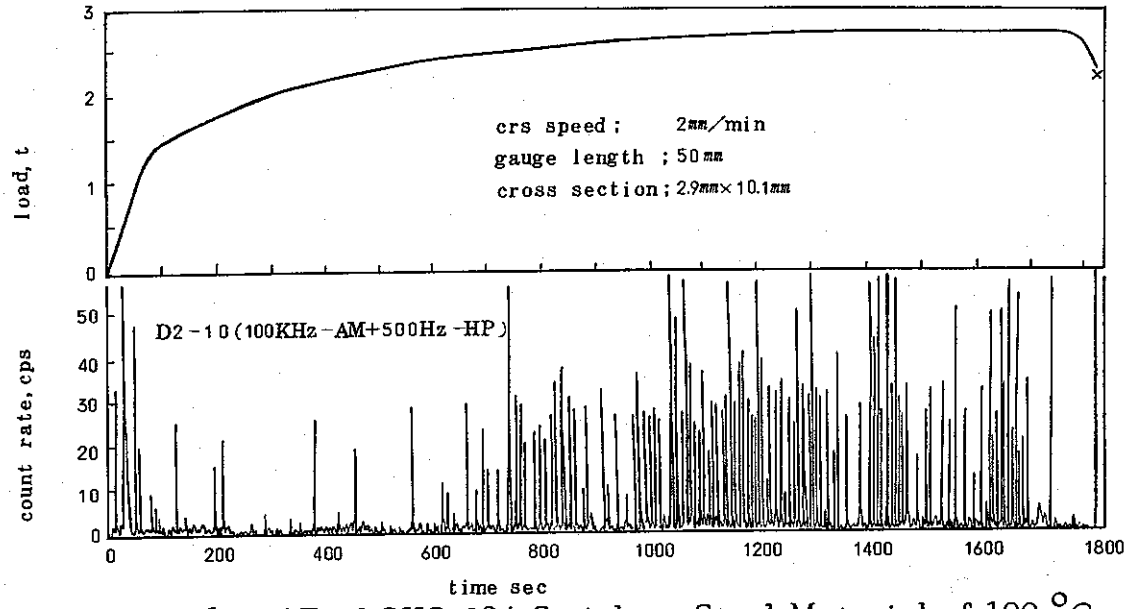

Fig. 2-6. AE of SUS 304 Stainless Steel Material of 100 °C, 1hr. Aging.

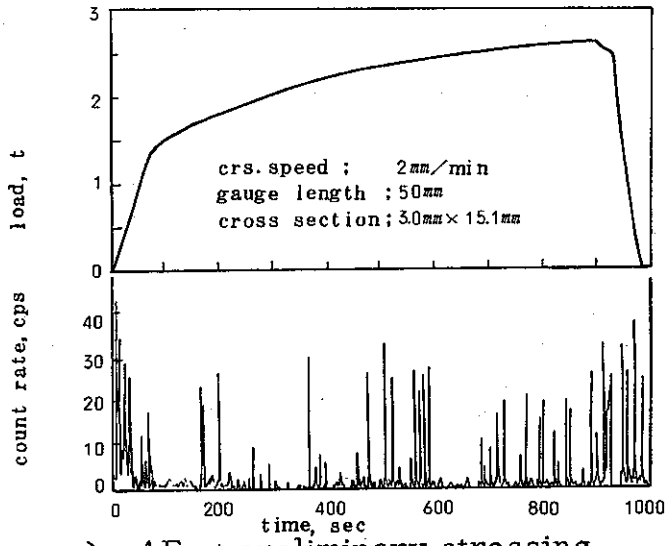

a) AE at preliminary stressing.

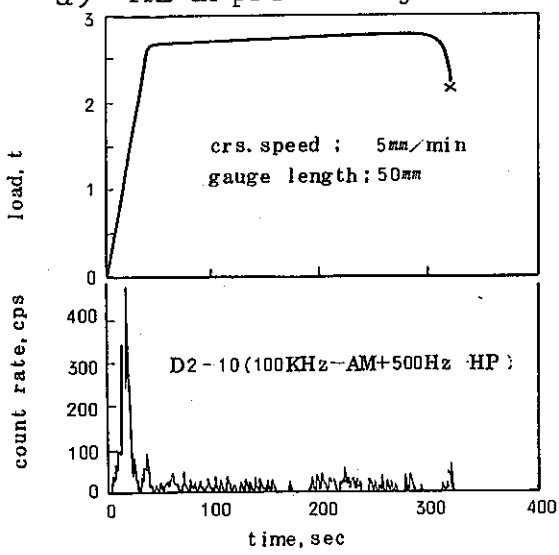

b) AE after preliminary stressing (after 100 °C, 1 hr. aging).

Fig. 2-7. AE of Stress Aged SUS 304 Stainless Steel Material

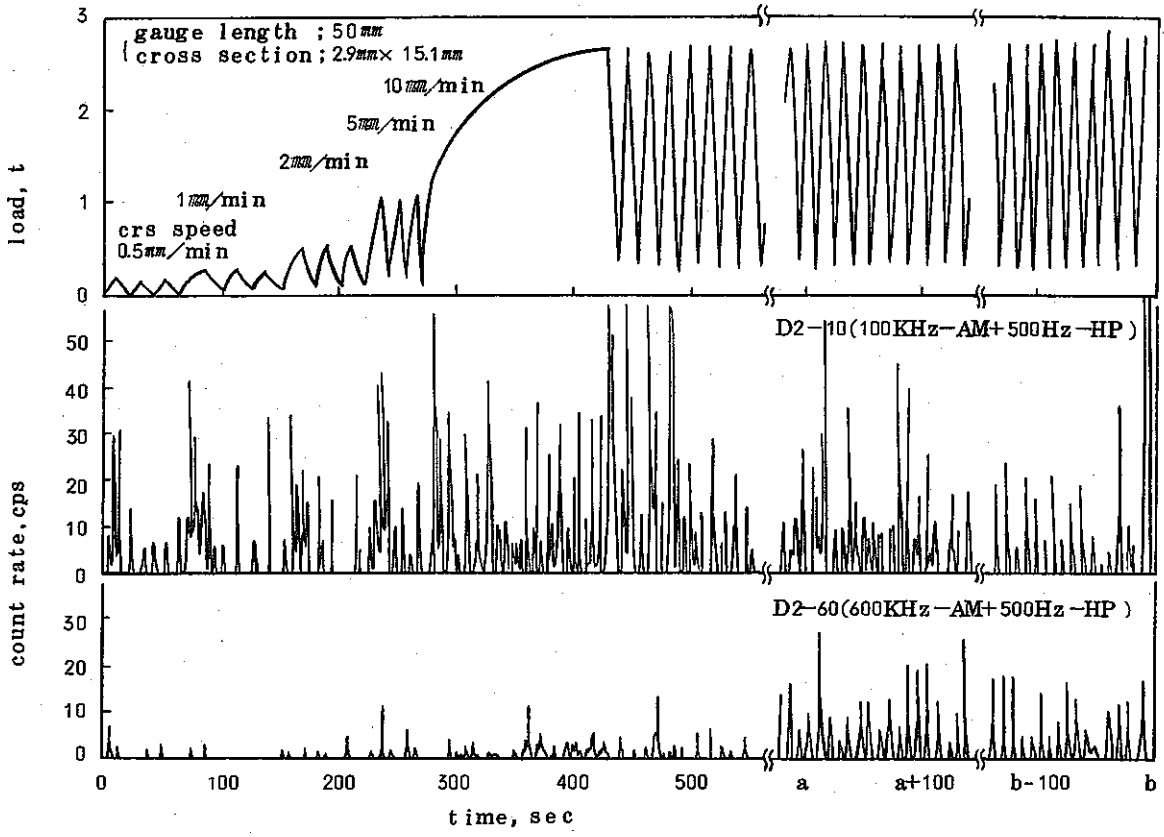

Fig. 2-8. AE under Repeated Load Test of SUS 304 Stainless Steel Material Annealed at 800 °C x 1hr.

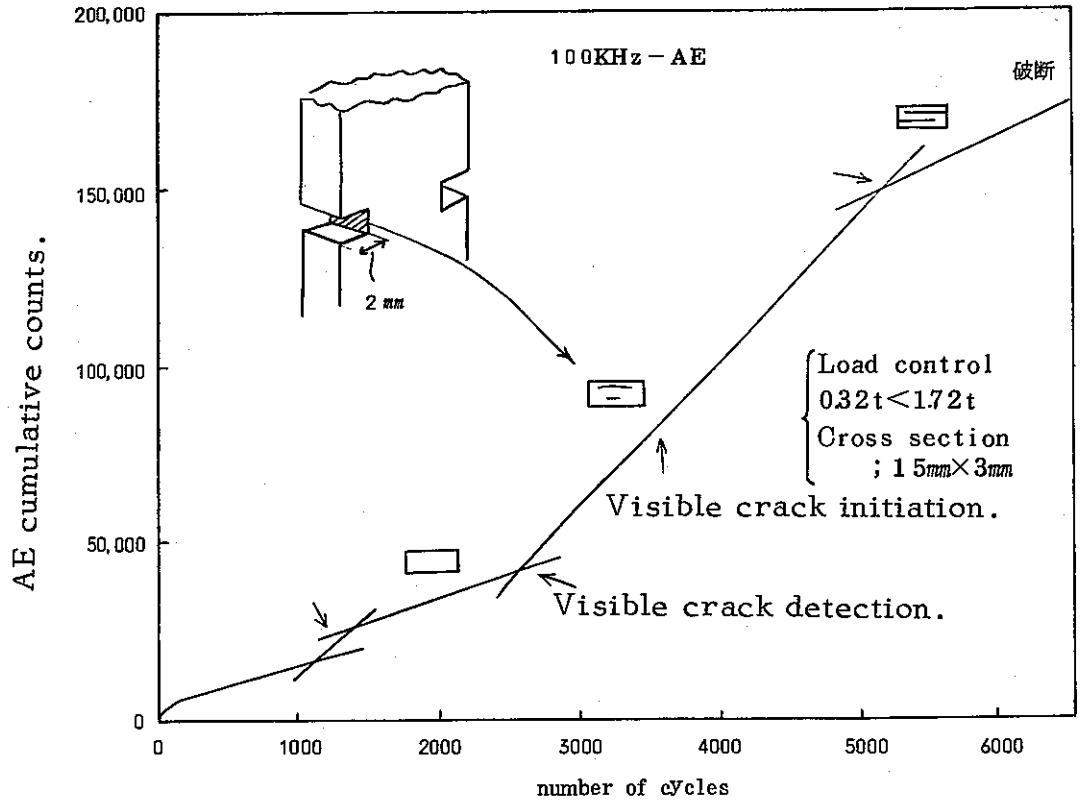

Fig. 2-9. AE Cumulative Total Counts Under Repetition Load Test of Material As Received with 2mm Notch.

c) AE signal with frequency of 100KHz corresponds to the pileup and breakaway of dislocations which are related to p plastic deformation. It is, however, considered that the high frequency element AE above 600KHz is corresponding to relatively macro-defects such as micro-fissures or cracks.

3. Results of Sound Monitoring During Fatigue Tests of Piping Components

3-1. Outline of Each Test

With a purpose to monitor by AE performance the behavior of the FBR piping elements under repetition of load, the following tests were undertaken.

1972

Feb. 2 - 5: BE-4 (12^BSch20 Long elbow room temperature test - av: -0.5t, amp: 3.3t load control)

Feb. 18 - 20: BE-5 (12^BSch20 Long elbow room temperature test - av: 0, amp: 40mm displacement control)

Mar. 4 - 5: BR-4 (12^B -6^BSch40Branch room temperature test - av: 0.5t, amp: 1.0t load control)

Apr. 12 - 17: BR-5 (12^B -8^BSch40Branch room temperature test - av: 0, amp: 2.0t load control)

May 2 - 4: BR-6 -(1) (12^B -8^BSch40Branch 550 °C test - av: 0, amp: 5mm displacement control)

May 13 - 25: BR-6 -(2) (12^B -8^BSch40Branch 550 °C test - av: 0, amp: 5mm displacement control)

Sept. 29 - 10.2: BR-6 -(3) (12^B -8^BSch40Branch 550 °C test - av: 0, amp: 7.5mm displacement control)

Fig. 3-1 a, b and c respectively show the shapes of BE tube, 12^B -6^B BR tubes, and 12^B -8^B BR tubes, and Table 3-1 represents the material of each test piece. Table 3-2 a, b, e, d, and

e show the examination data of BE-4, BE-5, BR-4, BR-5, and BR-6 specimens respectively. As to the welded materials, Table 3-3 gives the welding specifications and Fig. 3-2 the welding specification drawing.

Table 3-4 indicates the capacity of the hydraulic jack used to apply repeated load upon one end of the piping component fitted to the testing frame, and the capacity of the heater to keep the test specimen at 550 °C.

Table 3-5 represents the test conditions and the principal results of each of the tests. The following description introduces the outline of the respective tests based on the data given in said table.

(BE-4 Test)

This test was the first one performed to monitor piping structure by AE. The primary object was to see whether the AE technique which CRIEPI had applied to small size test pieces was effectively applicable to a large-size structure. The AE monitoring of this test, although it left some problems showed more or less satisfactory performance.

Observations of fatigue failure and acoustic emission were as follows: In the vicinity of 3935 cycles, AE signal count-rate increased, and at 4322 cycles, the operation of the test equipment was stopped. A subsequent observation of the test piece revealed a penetrated crack on one side of the bend, which was then cut open for a closer study, of which result was that there were also seen a number of small fissures of several millimeters inside the opposite part of the penetrated crack.

The fact that AE reacted sensitively to the development of

the crack during the test was considered due to the location of the AE element which fortunately was fitted at a position directly above the point where the crack occurred.

(BE-5 Test)

This test had for its purposes to confirm the reproducibility of the monitored AE data of the proviously tested BE-4, and to investigate the difference in the AE count rates of the previous load controlled test and the displacement controlled test of this time. Also, it was a secondary purpose to see the detection difference by placing the AE element at a location away from the crack.

This test has reconfirmed the previous finding that the AE count-rate increased along with the process of crack initiation and its penetration. But as a displacement control was employed this time for the test control method, there was seen no such remarkable AE signal changes as in the case of the previous BE-4 test.

As to the location of the AE element, it was found that a sufficient AE detection was possible even it was away from the crack by some 2 or 3 meters.

Observations of fatigue failure and acoustic emission were as follows: When a crack-gauge was adhered to the outer-surface of the test piece at 10000 cycles, the output showed an increase. At 10980 cycles, a crack penetration examination performed by means of an air-pressure revealed that there was already a penetration taken place. The destructive examination after test exposed no visible crack on the opposite side unlike in the case of BE-4 test.

(BR-4 Test)

The 20mmϕ AE element for a small-size tensile test had suffered a damage during the previous test, a 10mmϕ AE element was employed as a replacement. Because of this, the output signal - noise S/N ratio declined, which made it difficult to perform a sensitive detection of AE originating from cracks on piping structure. Also, when compared with the previous bend-pipe tests, less sufficiently effective result was obtained as to the crack development monitoring by AE count-rate because of the decline of AE amplitude and AE count-rate in this and the subsequent branch pipe tests. Particularly, in this test, a visible crack was detected by a color check in the range of $+60^{\circ}$ - -30° of the fillet on the branch side. But no clear change in AE count-rate was observed around this cycle. At 6896 cycles, crack penetration was observed. While the AE count-rate had shown a trend of slight rise from about 6700 cycles, this was not as conspicuous as it was in BE test.

(BR-5 Test)

As no change in AE count-rate was observed before and after the detection of a visible crack during the previous BR-4 test, several improvements were incorporated to heighten the sensitivity of the measuring system for this test. But this actually affected adversely and resulted in further deterioration in S/N ratio. Because of this, external electrical noises interfered with the AE signal makingit difficult to discriminate, and thus no satisfactory AE monitoring was possible.

Observations of fatigue failure were as described below;

At 18,250 cycles, a visible crack occurred, and a color

check at 18,500 cycles exposed fatigue cracks at a point near the upper left $+45^{\circ}$ and near the lower left 45°, and an air-pressure test at 48,240 cycles confirmed a crack penetration at a point near the upper right -45°.

(BR-6 Test)

This test was made under a high temperature of 550 $^{\circ}$C with a heater applied to the piping element which was wrapped with an insulation material to keep it heated. For the detection of a visible crack, the operation of the test equipment had to be temporarily stopped so that the heater and the insulation material could be removed for examination. For this reason, this test was conducted in three stages; namely the first stage upto 10,000 cycles, the 2nd stage to 100,000 cycles, and the third stage to 140,000 cycle where an increase of displacement amplitude resulted in a rupture of the test specimen.

For the AE detection under high temperatures, a waveguide method was employed. For the AE monitoring in the third stage, the AE count-rate and its cumulative total counts were counted together by a scaler, and it proved to be a good method of AE monitoring to display the crack propagation characteristics.

The AE signal emitted in a fatigue test of a piping element under high temperature differs conspicuously from that under room temperature. Both the amplitude and the count-rate are higher in the former. Thanks to this, and helped by the improvement of the measuring system, the AE monitoring of this test obtained a satisfactory result.

Observation of piping element at 10,000 cycles and 100,000 cycles found no crack initiation. But at the third stage, where

the displacement amplitude was increased, the AE performance changed in the vicinity of about 103,000 cycles and it was thought a crack had taken place. At 140,000 cycles, the test equipment operation was stopped for examination of the test specimen which then showed a crack penetration.

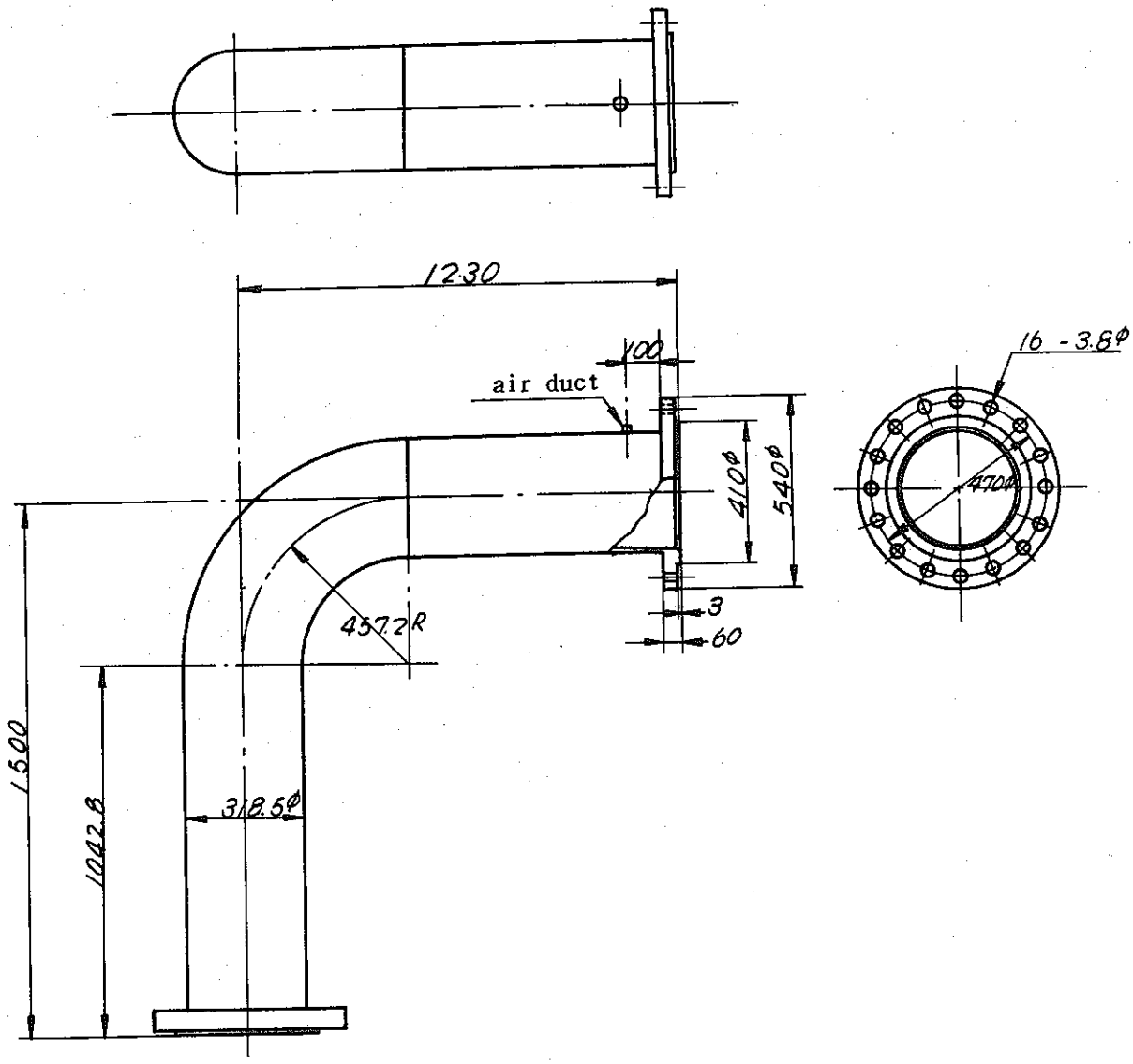

Fig. 3-1 a) Configuration of Bend Tube

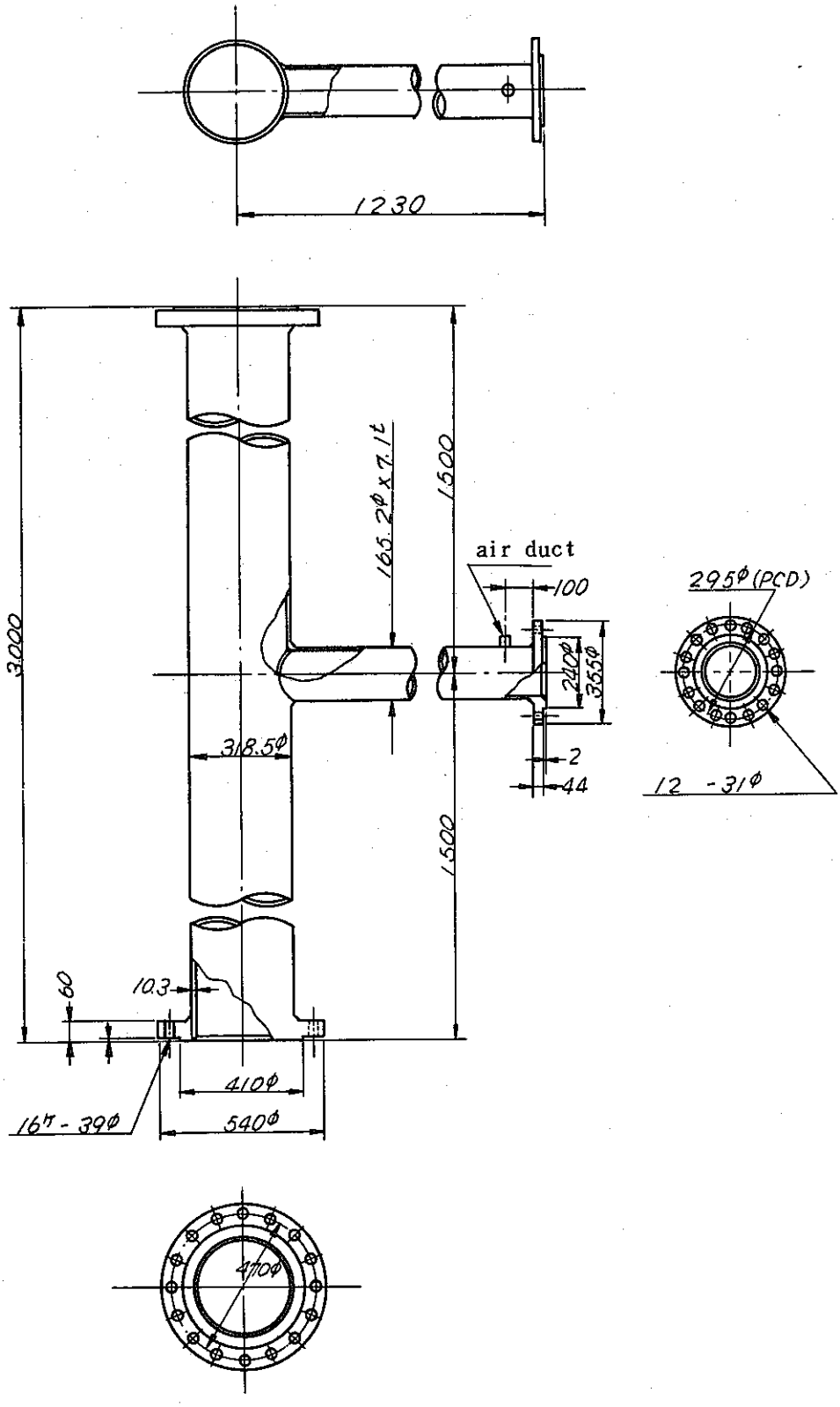

Fig. 3-1 b) Shape of Branch Tube (12B - 6B)

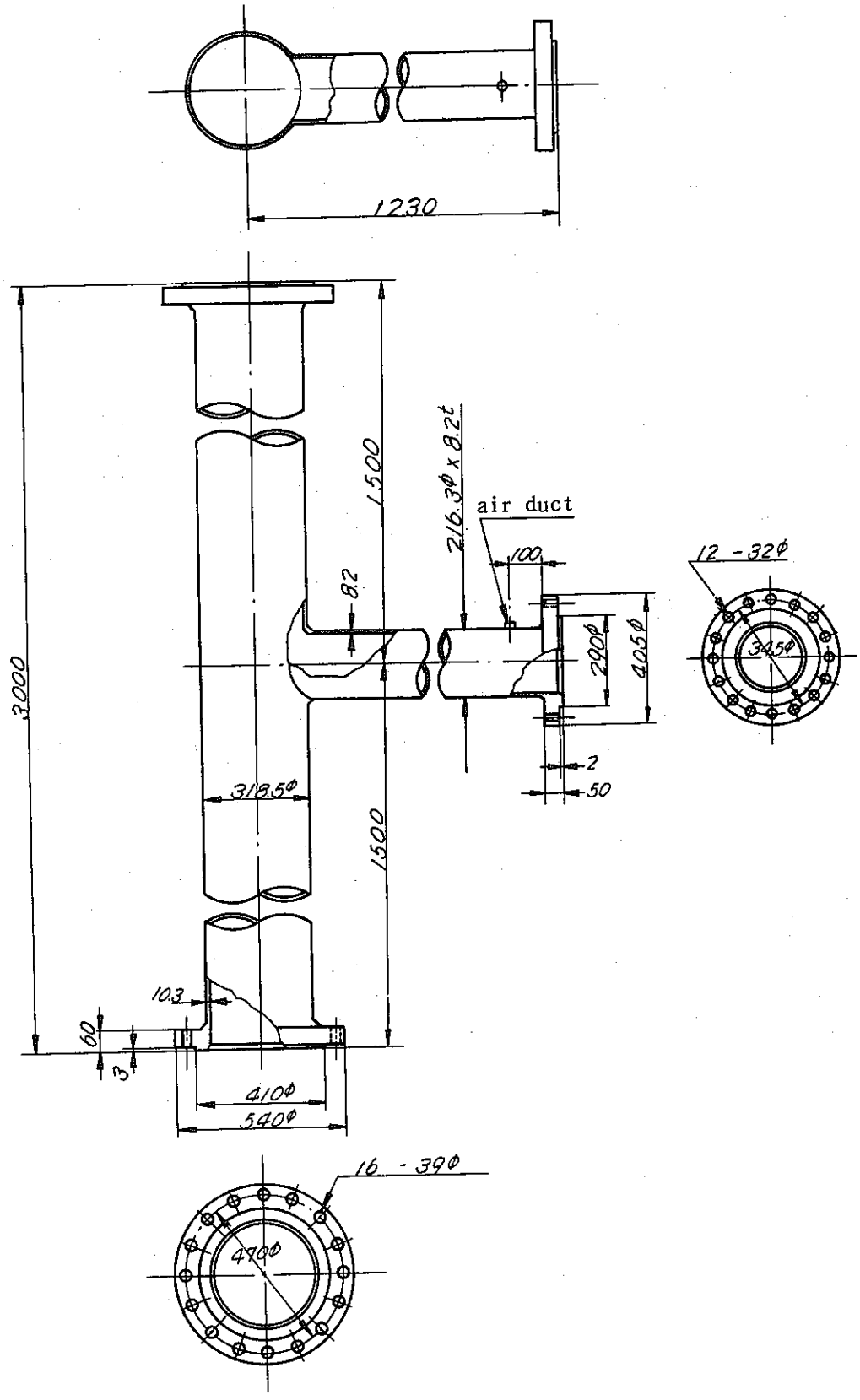

Fig. 3-1 c) Shape of Branch Tube (12B - 8B)

Table 3-1. Material List of Test Pieces

Material / Item	BE-4, 5	BR-4	BR-5, 6
Bend Tube	Straight SUS304 TP Bend SUS304 TP		
Flange for Bend Tube	SS41PL		
Branch Tube		Main SUS304TP Branch SUS304 TP	SUS304TP SUS304TP
Flange for Branch Tube		Main SS41PL Branch SS41PL	SS41PL SS41PL
Ventilation Hole	SUS304TP	SUS304TP	SUS304TP

Table 3-2 a) Examination data of BE-4 Test Specimen

Test No.	Size	Hydrostatic Test 25 (Kg/cm²)	Surface & Dimensions	Description of Test: Flattening	Expansion	Flaring	Flange	Bending Crush
	318.5×6.5×2000	Good	Good	Good				

Test No.	Tensile Properties: Yield Point (Kg/mm²)	Tensile Strength (Kg/mm²)	Elongations (%)	Chemical Analysis (%): C	Si	Mn	P	S	Cu	Ni	Cr	Mo
		63	61	0.07	0.72	0.91	0.024	0.019		8.61	18.04	

Table 3-2 b) Examination data of BE-5 Test Specimen

Test No.	Size	Hydrostatic Test 25 (Kg/mm²)	Surface & Dimensions	Description of Test				
				Flattening	Expansion	Flaring	Flange	Bending Crush
	3 18.5×6.5×4000	Good	Good	Good				

Test No.	Tensile Properties			Chemical Analysis (%)								
	Yield Point (Kg/mm²)	Tensile Strength (Kg/mm²)	Elongations (%)	C	Si	Mn	P	S	Cu	Ni	Cr	Mo
		68	64	0.07	0.74	1.65	0.29	0.008		8.78	18.57	

Table 3-2 c) Examination data of BR-4 Test Specimen

Test No.	Size	Hydrostatic Test 25 (Kg/cm²)	Surface & Dimensions	Description of Test				
				Flattening	Expansion	Flaring	Flange	Bending Crush
	318.5×10.3×3000	Good	Good	Good				
	165.2×7.0×4000	Good	Good	Good				

Test No.	Tensile Poperties			Chemical Analysis (%)								
	Yield Point (Kg/mm²)	Tensile Strength (Kg/mm²)	Elongations (%)	C	Si	Mn	P	S	Cu	Ni	Cr	Mo
		62	61	0.07	0.89	1.60	0.022	0.010		8.61	18.40	
		57	66	0.07	0.75	1.65	0.030	0.007		8.81	18.73	

Table 3-2 d) Examination data of BR-5 Test Specimen

Test No.	Size	Hydrostatic Test 25 (Kg/cm²)	Surface & Dimensions	Description of Test: Flattening	Expansion	Flaring	Flange	Bending Crush
	318.5×10.3×3000	Good	Good	Good				
	216.3× 8.2×1200	Good	Good	Good				

Test No.	Tensile Properties: Yild Point (Kg/mm²)	Tensile Strength (Kg/mm²)	Elongations (%)	Chemical Analysis (%): C	Si	Mn	P	S	Cu	Ni	Cr	Mo
		62	61	0.07	0.89	1.60	0.022	0.010		8.61	18.64	
		60	63	0.07	0.31	1.00	0.022	0.014		8.61	18.64	

Table 3-2 e) Examination data of BR-6 Test Specimen

Test No.	Size	Hydrostatic Test 25 (Kg/cm²)	Surface & Dimensions	Description of Test				
				Flattening	Expansion	Flaring	Flange	Bending Crush
	318.5×10.3×3000	Good	Good	Good				

Test No.	Tensile Properties			Chemical Analysis (%)								
	Yield Point (Kg/mm²)	Tensile Strength (Kg/mm²)	Elongations (%)	C	Si	Mn	P	S	Cu	Ni	Cr	Mo
		62	61	0.07	0.89	1.60	0.022	0.010		8.61	18.40	

Table 3-3. Welding Specifications

Flange

(BR) Welding rod D-316-16 Kobe Steel NC-36

1st layer	4.0 ϕ	D.C. Reversed Polarity
2nd layer	5.0 ϕ	"
3rd layer	5.0 ϕ	"
4th layer	5.0 ϕ	"
5th layer	5.0 ϕ	"

1st layer	3.0 ϕ	
2nd layer	3.0 ϕ	Two-layer weld

(BR) Welding rod D-316-16 Kobe Steel NC-36

1st layer	4.0 ϕ	D.C. Reversed Polarity
2nd layer	5.0 ϕ	"
3rd layer	5.0 ϕ	"
4th layer	5.0 ϕ	"
5th layer	5.0 ϕ	"
6th layer	4.0 ϕ	Total "
		Total 6-layer weld

1st layer	4.0 ϕ	One layer weld

T-Pipe's fillet weld

Welding rod D-308-16 Kobe Steel NC-38

1st layer	Argon arc welding (1.2 ϕ)	
2nd layer	3.2 ϕ	D.C. Reversed Polarity
3rd layer	4.0 ϕ	"
4th layer	4.0 ϕ	"
5th layer	3.0 ϕ	"

Total 5-layer weld

Elbow

Welding rod D-308-16 Kobe Steel NC-38

1st layer	Argon arc welding (1.2 ϕ)	
2nd layer	2.6 ϕ	D.C. Reversed Polarity
		Total two-layer weld

Table 3-4. Equipment Capacity

Item	Capacity	
Hydraulic Jack	Oil pressure	Max.200Kg/cm^2
	Load	Max.±50ton. Min.±10ton
	Displacement	Max.±100mm
	Repetition Speed	Mzx. $\frac{1200}{S}$ under load (S: stroke mm)
Heater	Capcity	3 KVA (200V single phase) x 6 -division, totalling 18 18KVA.
	Model	Fitting type to the test piece
	Control	On-Off control by the thermo-electric couple for each division

BR 12 B Flange

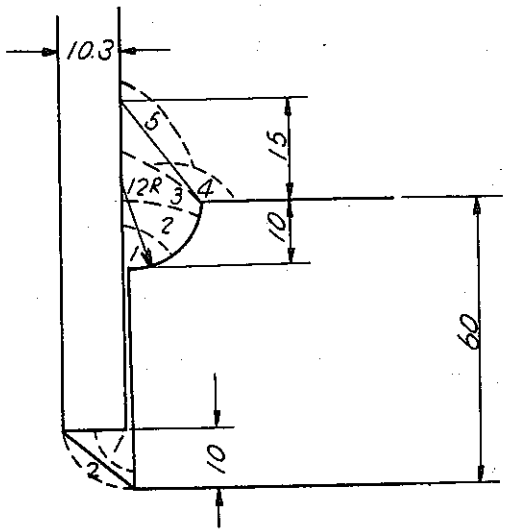

BE Flange

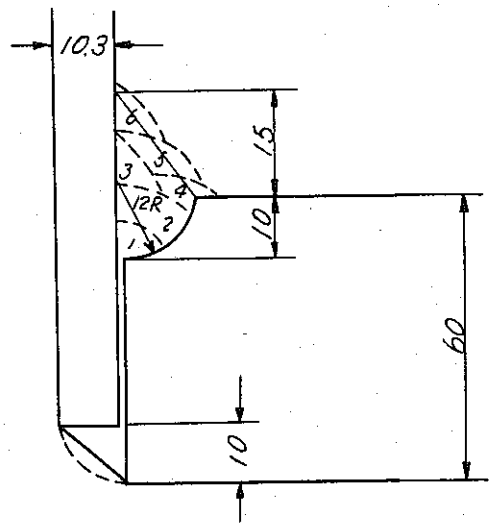

T-tube fillet

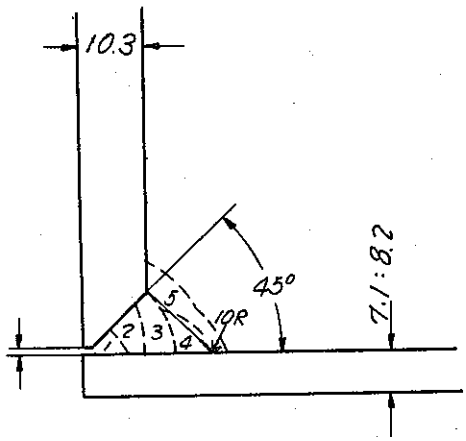

Elbow

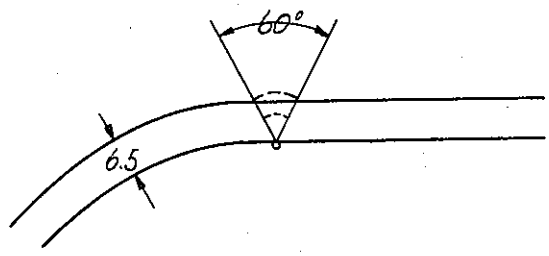

6B Flange

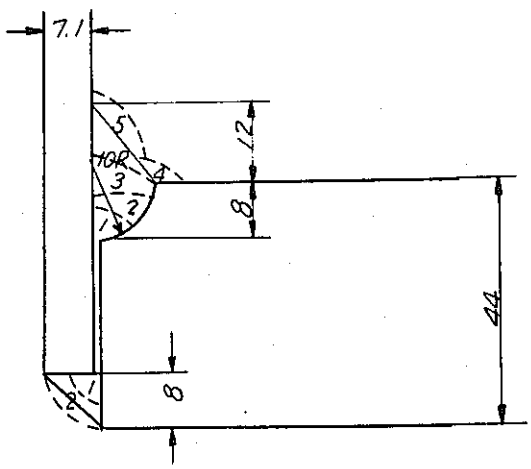

8 B Flange

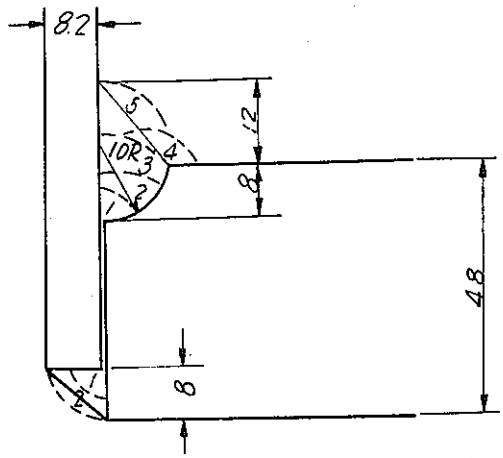

Fig. 3.2 Welding specifications.

Table 3-5. List of Fatigue Failure Tests of Piping Components

Test Specimen	BE-4	BE-5	BR-4	BR-5	BR-6(1)(2)	BR-6(3)
Test Temp.	Room Temp.	Room Temp.	Room Temp.	Room Temp.	550 °C	550 °C
Control Method	Load	Displacement	Load	Load	Displacement	Displacement
Control Vol. (Measured)	-4.2 ~ 2.0^t	-40 ~ 40 mm	0.0 ~ 1.92^t	-2.0 ~ 2.0^t	-4.0 ~ 5.0 mm	± 7.5 mm
Principle strain range	ε_c = 8350 μ	ε_c = 5652 μ	ε_I = 7875 μ	ε_I = 4631 μ		
	ε_t = 2800 μ	ε_t = 2326 μ	ε_{II} = 2305 μ	ε_{II} = 1013 μ		
Cycle Number N	4,322	11,000	6,896	49,915	100,000	(100,000 +) 40,000
Cycles to Visible Crack Detection Nc	(2.161)	(5.490)	4,233	18,496	(n/Nc=0.77)	(100,000 +) 3,000
Cycles to Crack Penetration N	4.322	10.980	6.89	48.240	(n/Nc=0.29 —	(100,000 +) 39,000
Crack Propagation Speed	Linear Approximation Plate Thickness Direction	—	(4000 N 7000) 0.002mm/cycle	(1800 N 47000) 0.0002mm/cycle —		
				(47000 N 48000) 0.0008mm/cycle —		

Measuring System	Load Displacement	Load Displacement	Load Displacement	Load Displacement	Load Displacement	Load Displacement
	Strain-gauge (2-axes x 22)	Strain-gauge (2-axes x 24)	Strain-gauge (3-axes x 13)	Strain-gauge (3-axes x 16)	High temp. strain-gauge (x 8)	High temp. strain-gauge thermoelectric couple
			Stress concentration gauge (x 1) One crack gauge (x 8)	Crack gauge (x 4)	Thermoelectric couple (27)	Smec gauge
AE Element	100KHz(20ϕ) 600KHz(20ϕ)	100KHz(10ϕx20ϕ) 600KHz(20ϕ)	100KHz(10ϕx3) 1MHz(10 ϕ)	100KHx(10ϕx2) 100KHz(20ϕ) 1MHz(20ϕ)	100KHz(10ϕ) For high temp. x 2	100KH(10ϕ) For high temp. x 2
AE Element Fitting	Direct	Direct	Direct	Direct + Waveguide	Wageguide	Waveguide
AE Monitor Record	Count-rate	Count-rate	Count-rate	Count-rate	Count-rate	Count-rate + Cumulative Numbers
Result of AE Monitor	Fairly good	Fairly good, but Correspondability not sufficient	S/N ratio not very good due to 10ϕ probe	Bad as electrical noises picked up	Good	Good
Load	6.2 t	5.88 t	1.92 t	4.0 t		
Displacement	110 mm	80 mm		15.0 mm	9.0 mm	15.0 mm
Stress range (by Sec.III)	$S=109kg/mm^2$ $K_e^P S_p=364kg/mm^2$	$103kg/mm^2$ $345kg/mm^2$		$204kg/mm^2$	$102kg/mm^2$	$163kg/mm^2$
Strain range (by Sec.III)	$S_p/E = 5540$	5255		8400	5280	8400

3-2. Bend Tube, BE-4 Test

(1) Purpose of AE monitoring

In this test, the AE measurement was performed for the following purpose:

a) To evaluate the applicability of the AE measurement experience and the AE monitoring system for the small test pieces of SUS 304 stainless steel.

b) To grasp the environmental noises at the time of a fatigue test on piping components.

c) To find the adequate structure of a sound probe and the method of its fitting to a test specimen.

d) To grasp the AE performance changes in the fatigue test of bend tube.

(2) AE Monitoring System

Fig. 3-3 shows the AE monitoring system employed in this test. The sound probes used for the test were 20mmϕ PZT sensor with resonance at 100KHz and 600KHz. They were bound by brass bands to the mid-part of (the bending section of) the bend tube (refer to Fig. 3-3) with a piece of rubber coated with silicon grease between the band and specimen.

(3) Fatigue Test and Its Development

The following Table 3-6 represents the progress of the test:

Table 3-6. BE-4 Test Development

Time	Load	Frequency	Cycle Counts
Feb. 4	Tons	cpm	
12°45'	-0.5 - 0.5	5	1
12°50'	-1.0 - 1.0	5	6
12°55'	-2.0 - 2.0	5	11
13°00'	-4.0 - 2.0	5	16
13°05'	-4.5 - 3.5	5	21
13°05'	-4.0 - 3.0	5	23
13°15'	-4.0 - 3.0	10	57
13°25'	-3.8 - 2.8	5	129
14°10'	-4.2 - 2.0	5	359
Feb. 5			
3°-	-4.2 - 2.0	5	4,307 (Surface crack detected)
4°00'	-4.2 - 2.0	5	4,322 (Crack penetrated)

(4) AE Measurement Results

a) AE Characteristics under Increasing Load Amplitude

Along with the stepwise increase of the load amplitude from ±0.5t, ±1.0t, ±2.0t, ±3.0t, and up to ±4.0t, both AE signals of 100KHz and 600KHz increased in their amplitude and count-rate. Due to the influence of Kaiser effect, the first cycle in each step of load had the highest AE counts, which, however, gradually declined later on. Fig. 3-4 represents the typical 100KHz AE count-rate patterns monitored under the ±2t and ±3t load amplitudes. Fig.

3-5 a) and b) show the amplitude distribution, obtained by PHA, of 100KHz AM signal recorded in the magnetic tape under each load amplitude.

b) AE Characteristics at Constant Load Cycling

The AE count-rate was comparatively large at the beginning, of 5 cpm 3 ton fully reversed constant load cycling, which was thought as related to the plastic deformation. Then it declined at about 1500 cycles, and became sporadic around 3000 cycles. Around 3800 cycles, AE count-rate gradually rose again, and after 4000 cycles, it very rapidly increased. At 4307 cycles, a crack was observed.

Fig. 3-6 shows the monitored data of the 100KHz AE count-rate, and Fig. 3-7 a) and b) give the PHA-analyzed data of the AE records 100KHz AM component. It evidently indicates the increase of AE amplitude and its count-rate along with the number of load cycling.

3-3. Bend Tube, BE-5 Test

(1) Object of AE Monitoring in this test

In the previous BE-4 test, the object of the test was to check on the adaptability to the FBR Piping Components of the AE technique which had been tried with small test pieces. The result of the test was generally satisfactory, and this time, the test was aimed at the following subjects:

a) Study on the reproducibility of AE monitoring using the same measuring system as used in the previous test.

b) AE performance difference in the load controlled test and the displacement controlled test of bend tubes.

c) Influence of the sound probe fitting position.

Fig. 3-3. Schematic Drawing of AE Monitoring System In BE-4 Test

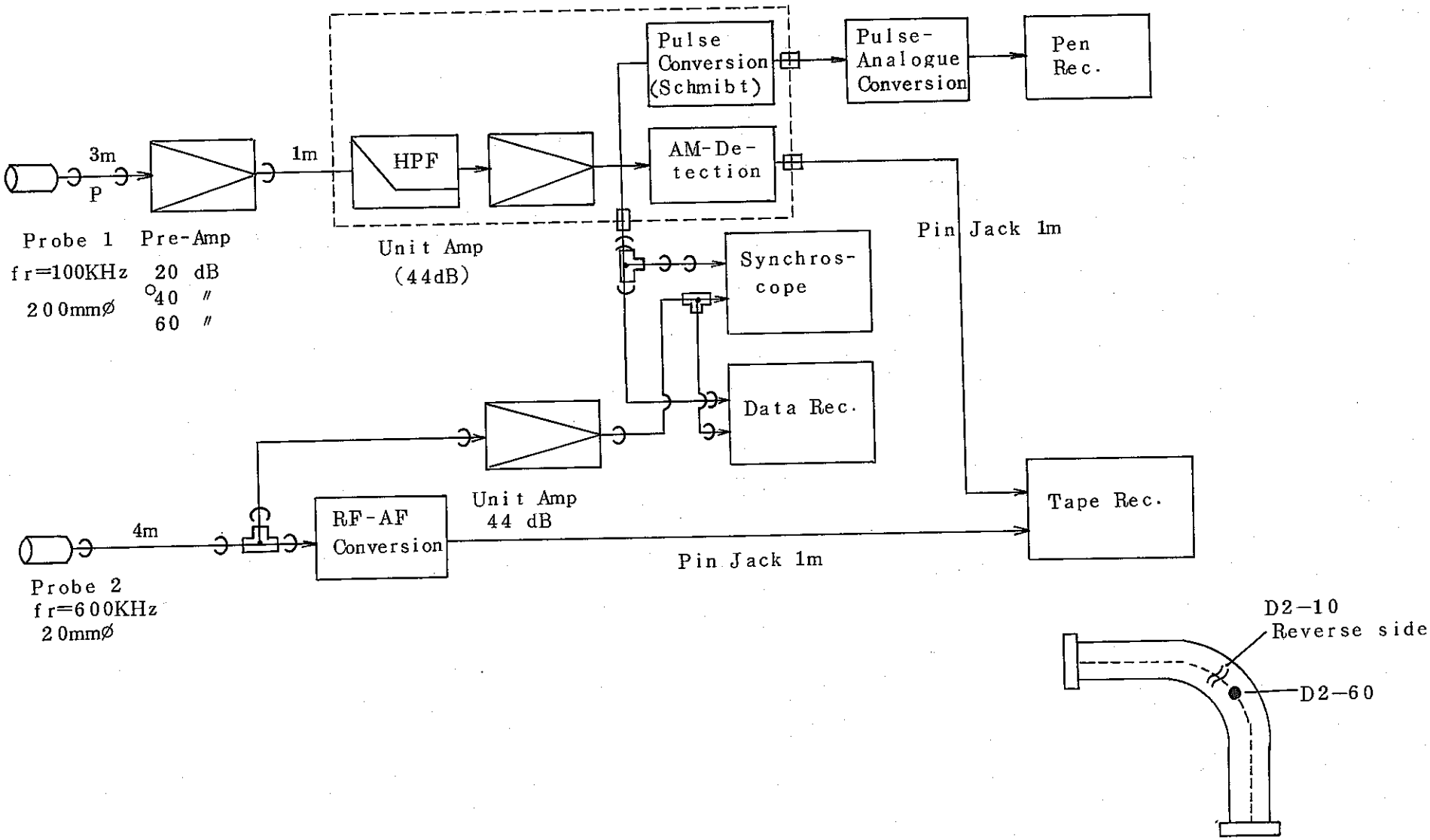

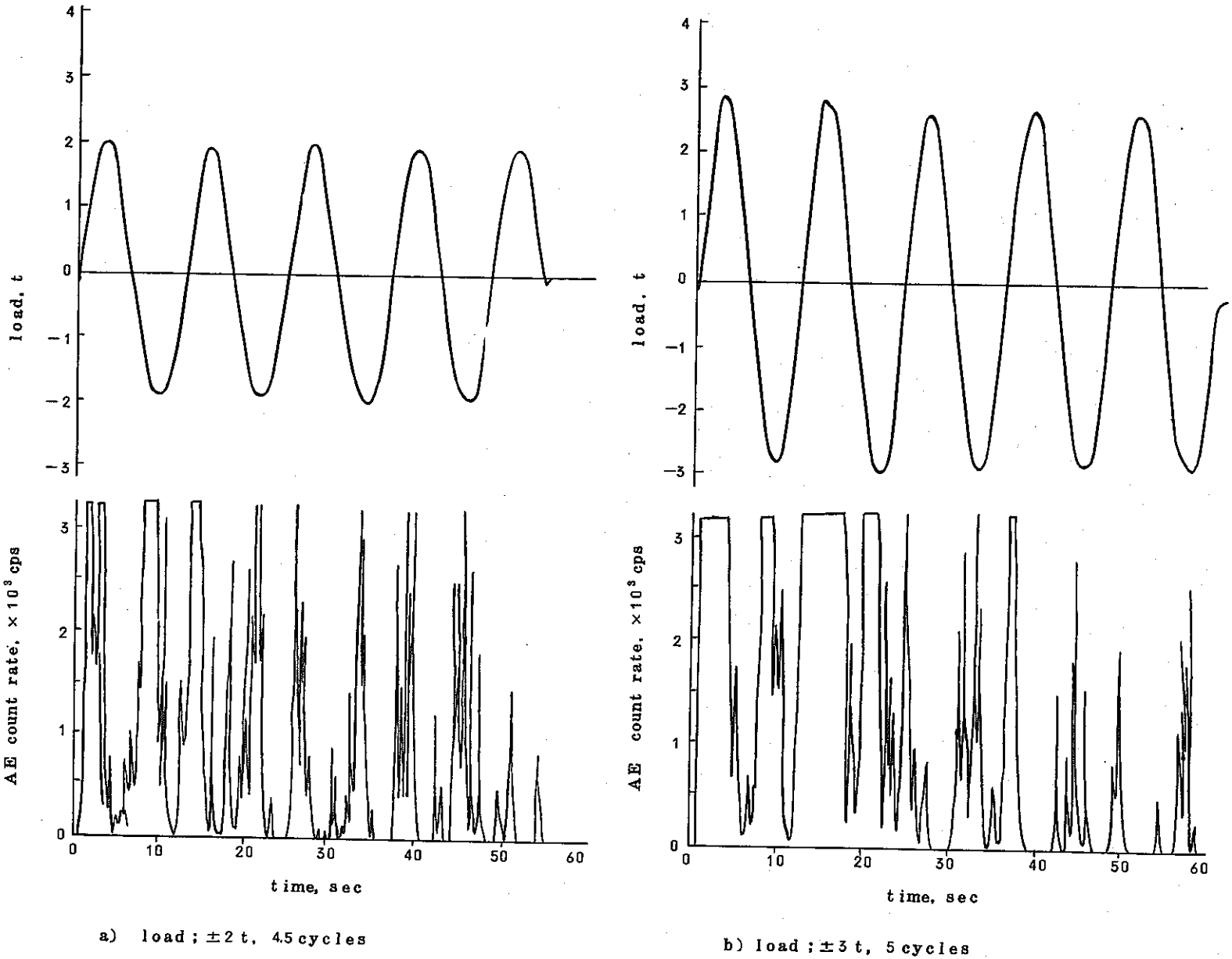

a) load ; ±2 t, 4.5 cycles

b) load ; ±3 t, 5 cycles

Fig. 3-4 AE Count-Rate Monitoring At Initial Load Increase

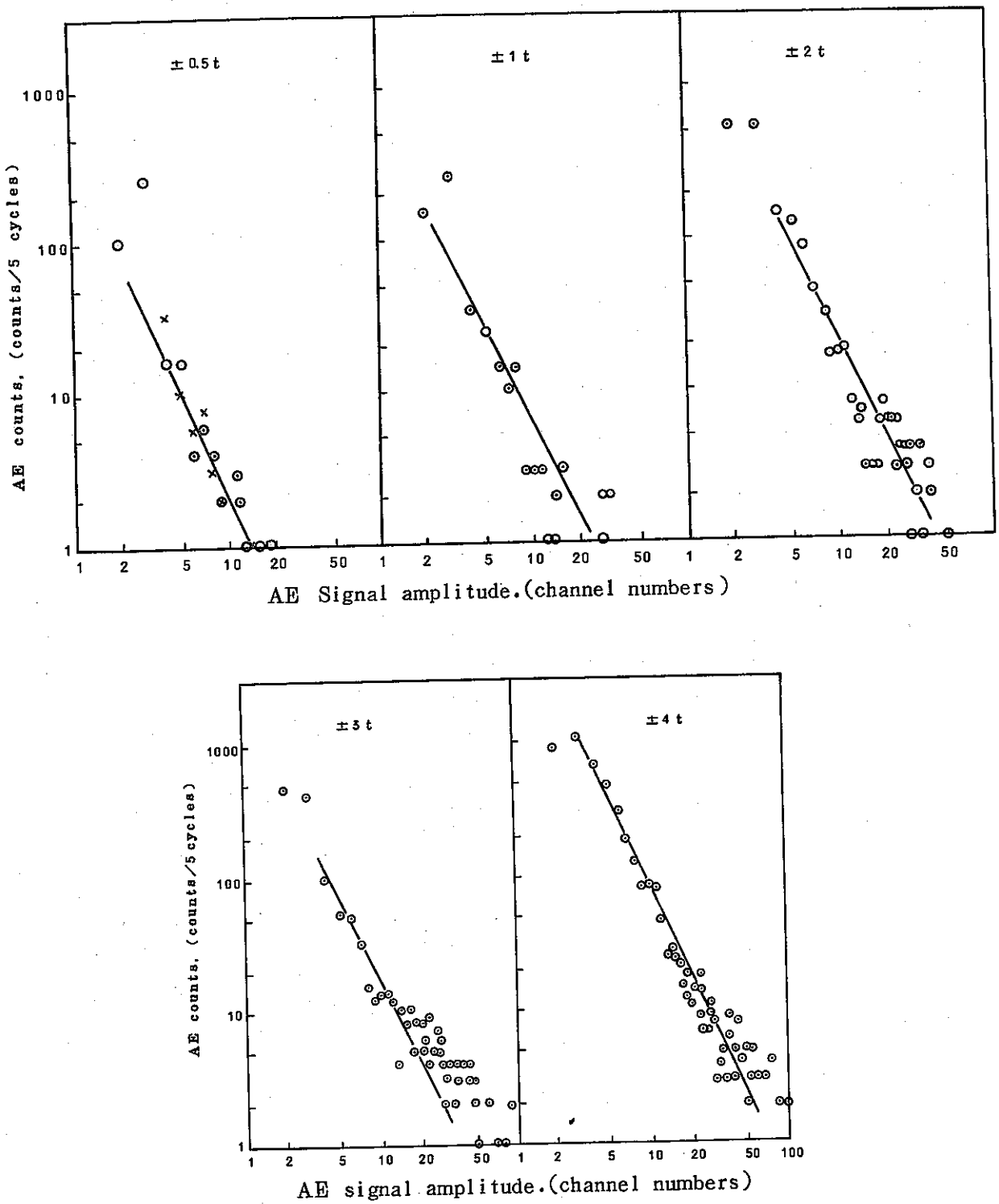

Fig. 3-5 Relation Between AE Amplitude and Count Rate Under Load Amplitude Increase in BE-4 Test

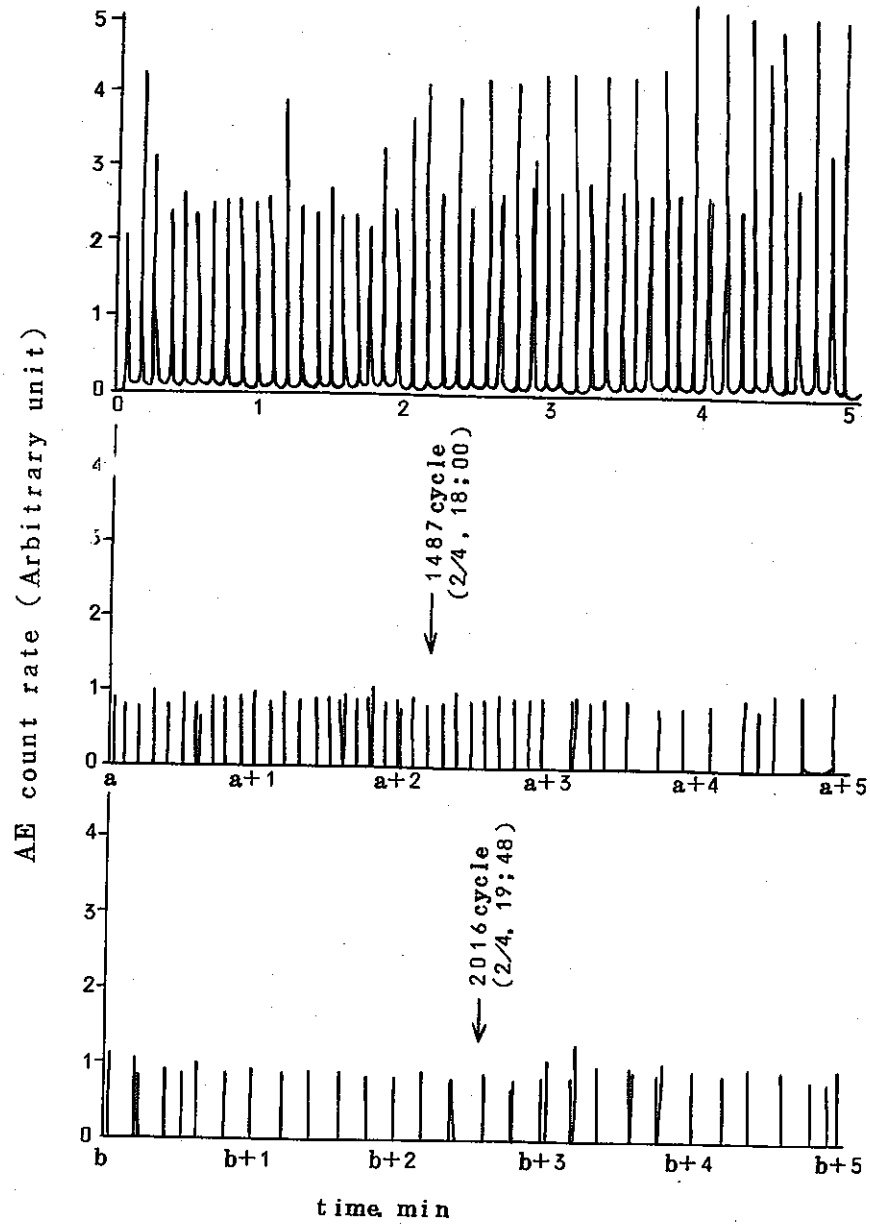

Fig. 3-6 a) AE Count Rate Graph Under Constant Load Cycle in BE-4 Test (An Example) (1)

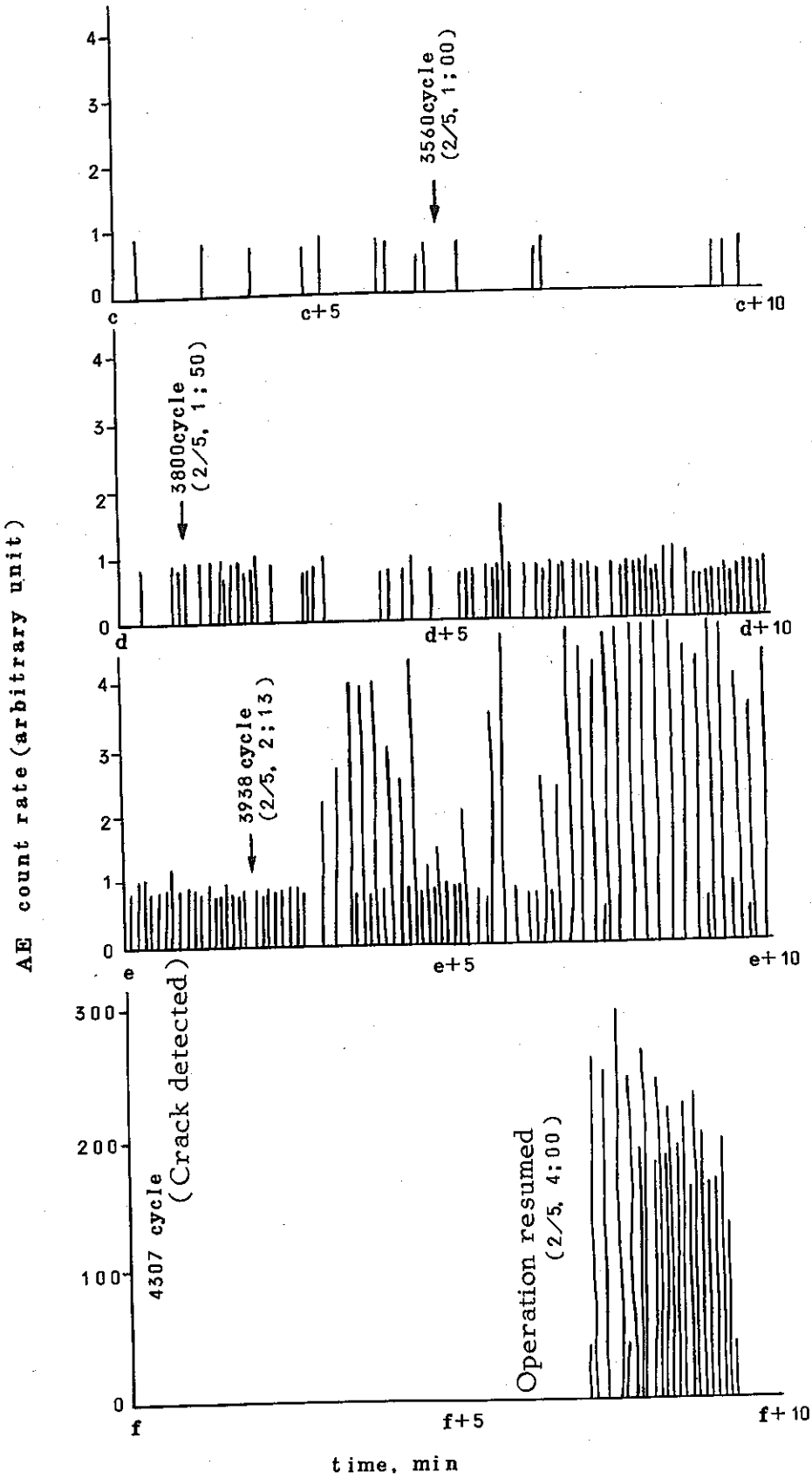

Fig. 3-6 b) AE Count Rate Graph Under Constant Cycle in BE-4 Test (Example 2)

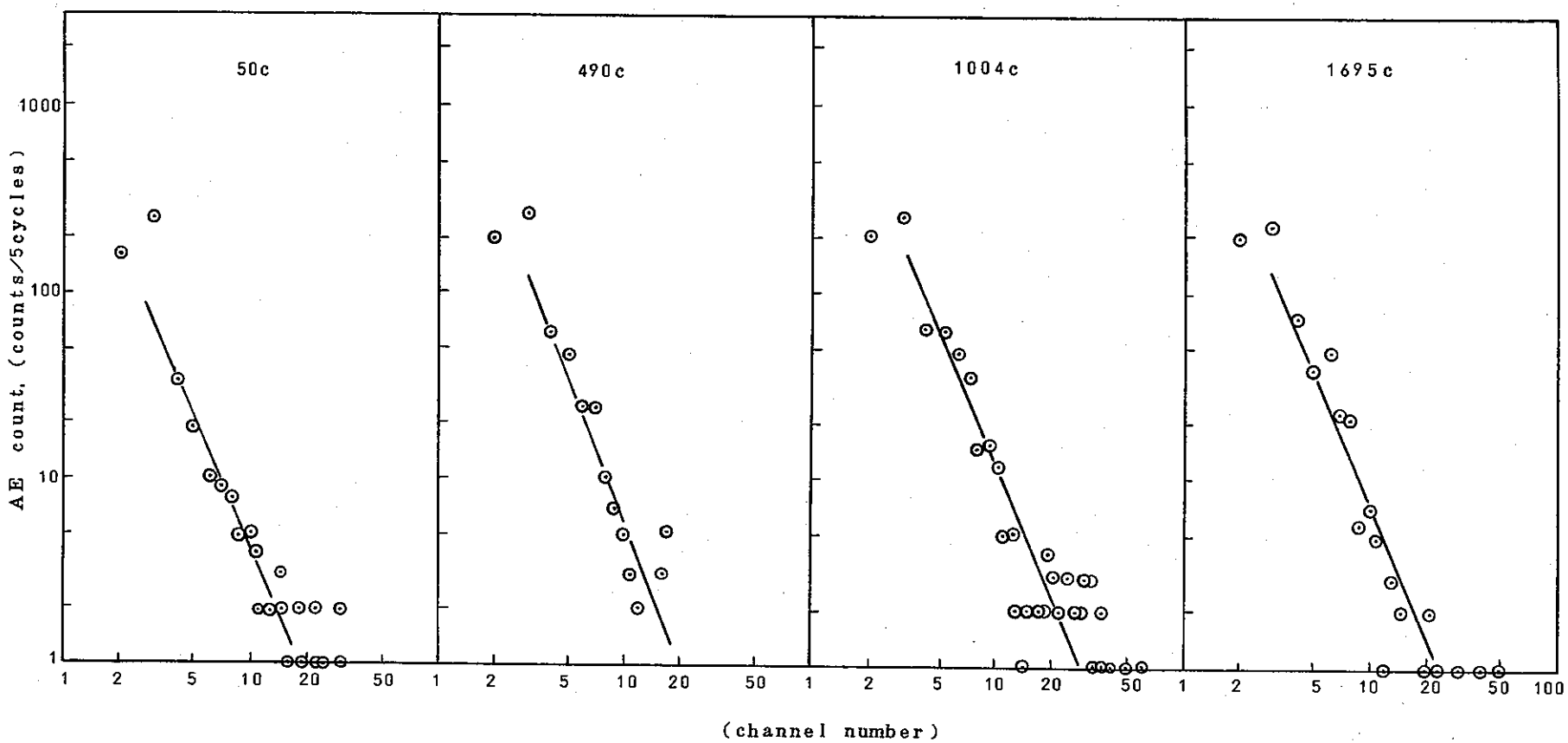

Fig. 3-7 a) Relation Between AE Amplitude and Count-Rate Under Constant Load Cycle in BE-4 Test (1)

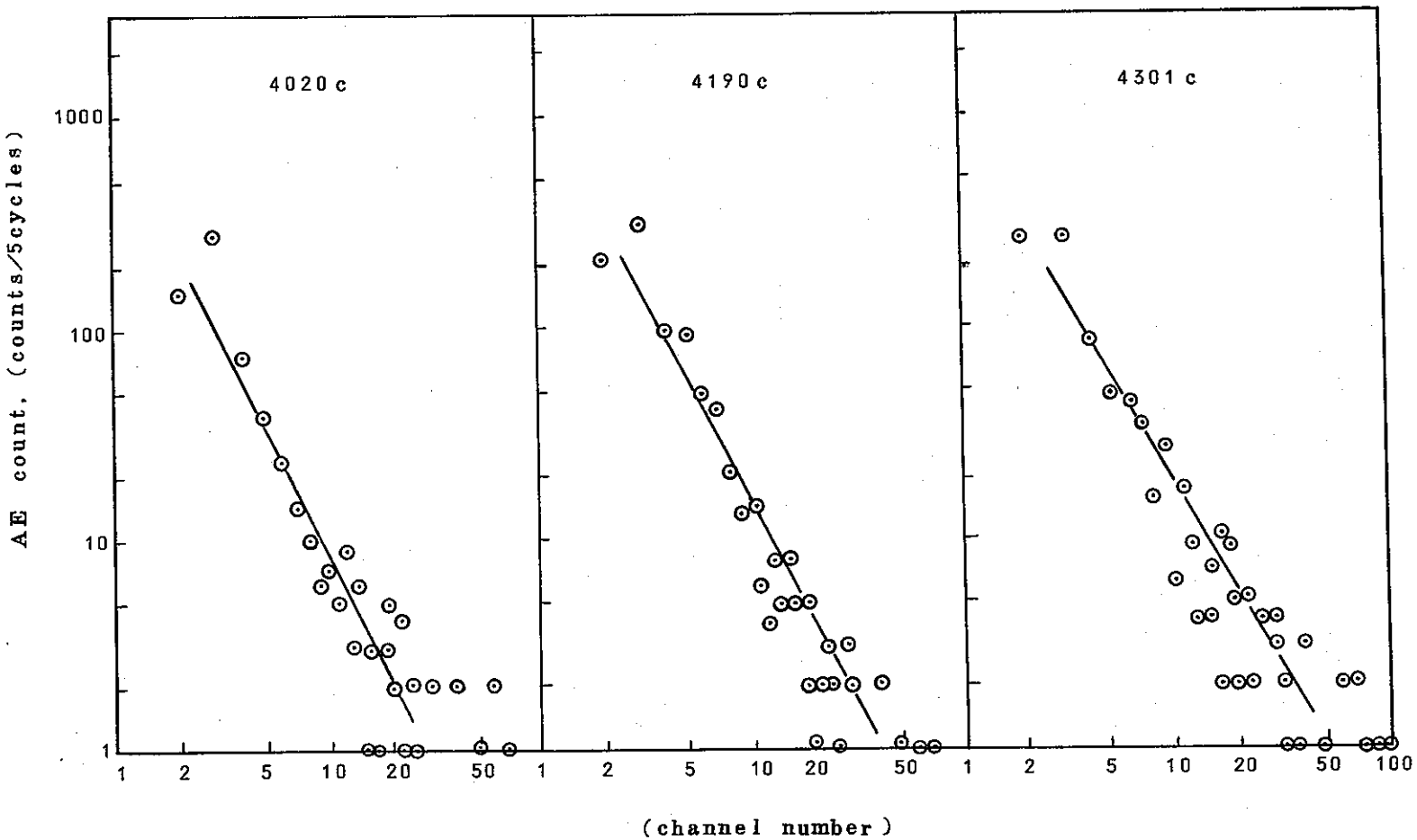

Fig. 3-7 b) Relation Between AE Amplitude and Count-Rate Under Constant Load Cycle

(2) AE Monitoring System

The schematic drawing of the AE monitoring system employed in this test is as shown in Fig. 3-8. The sound probe and the method of its fitting to the test specimen were identical as in the case of the previous test. A 100KHz resonant probe of 10mmϕ was fitted at the location about 35cm above the lower fixed end of the bend tube in order to check on the influence of positional difference.

(3) Development of Fatigue Test

The development of this test is as shown by Table 3-7.

Table 3-7. BE-5 Test Development

Time	Displacement	Frequency	Cycle Counts
Feb. 18	mm	cpm	
–	± 5	5	4.5
–	± 10	5	9
–	± 20	5	13.5
–	± 30	5	18
–	± 40	5	30
20°00'	± 40	8	365
–	± 40	5	687
Feb. 19			
16°21'	± 40	8	6,600
23°30'	± 40	8	10,000 (Temporarily suspended)
Feb. 20			
2°34'	± 40	8	10,001 (Resumed)
20°34'	± 40	5	10,548 (Resumed after color check)
22°00'	± 40	5	10,980 (Crack penetration)
–	± 40	5	11,000 (Test finalized)

(4) Results of AE Monitoring

a) When the displacement amplitude was increased during the preliminary cycles, AE count-rate and its amplitude also increased as in the case of BE-4 test.

b) In the constant cycling, the AE of 100KHz component was high in its count-rate at the beginning of the test, and later, in the midway of the test, the count-rate declined. But in the stages of crack initiation and its propagation, occasional peaks of AE count-rate were observed, and as nearing to the crack-penetration, the count-rate again rose and the amplitude frew larger. These trends were also seen in the case of BE-4 test. Thus, its reproducibility was confirmed satisfactorily.

c) Also, the AE counts of 600KHz component showed the similar phenomenon as in the case of 100KHz AE. But in the midway of the test, AE count-rate conspicuously declined while it rose at the finishing stage. The count-rate, however, was lower when compared with that of 100KHz component.

d) Near crack initiation, the output increase of the AE count-rate monitoring system was not as conspicous as in the case of the previous BE-4 test. As the reason, it is considered, besides the problems of the probe location and its sensitivity, that the process of the crack development in this displacement controlled test was different from that of the previously performed load controlled test.

e) AE detection difference due to the difference in probe position was examined by putting sound probes at the mid-

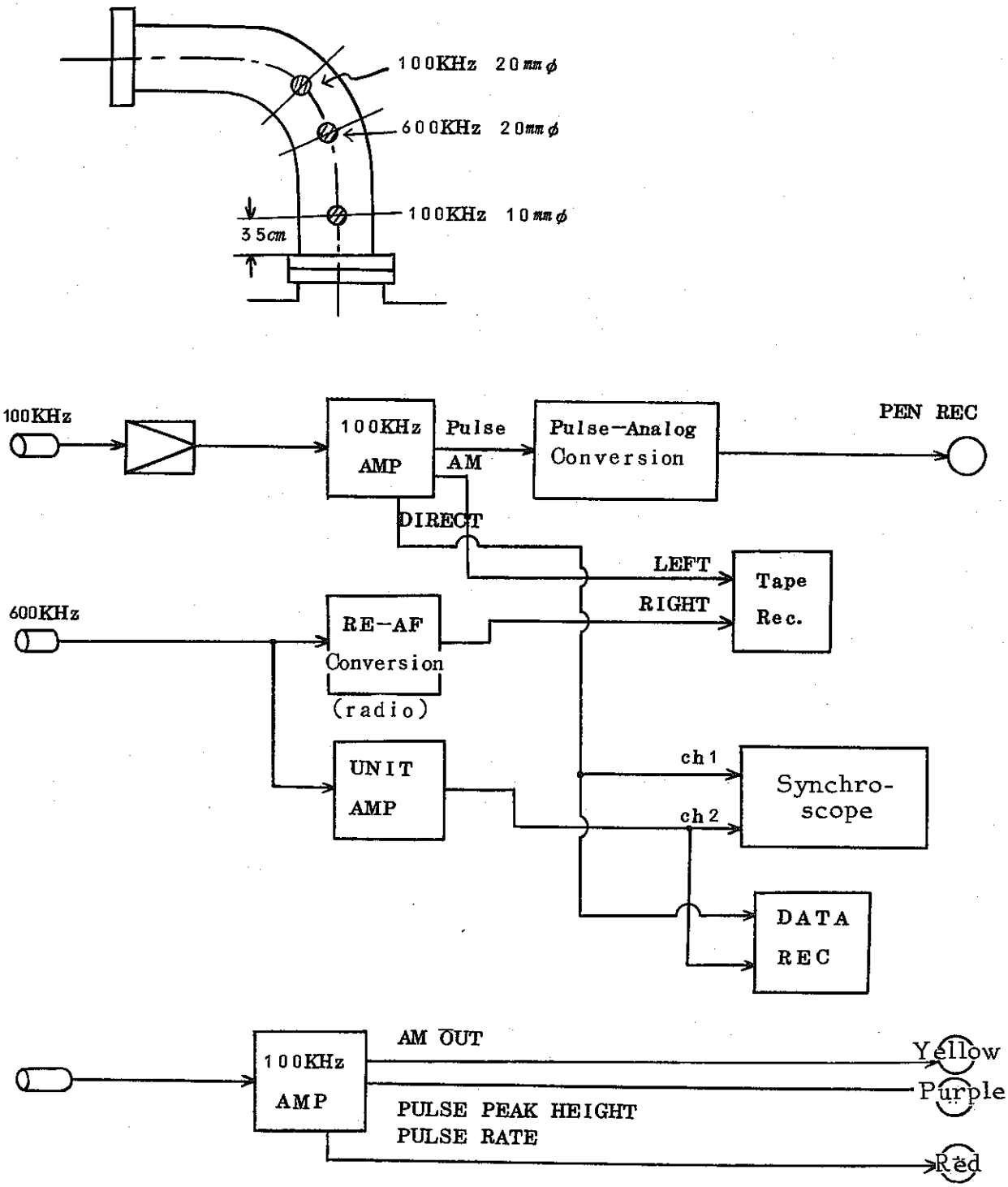

Fig. 3-8 AE Monitoring Schematic Drawing for BE-5 Test

part and the lower end of the piping. The results showed a very little difference between both AE data and it was found out that even at 2 - 3 meters distance, AE detection was possible.

3-4 Branch Tube, BR-4 Test

(1) Purpose of AE Monitoring in This Test

a) To check on the difference of AE performance between BE test and BR test.

b) Application of a closed type probe.

(2) AE Monitoring System

Fig. 3-9 represents the schematic drawing of the AE monitoring system. The sound probes which were employed this time were of 10mmϕ since the previously used 20mmϕ type became unusable. Of the four kinds of probes A, B, C, and D, as shown in Fig. 3-9, A and B are of a closed type which has a sensor enclosed in a brass housing. This closed type probe, although, is different in construction from the conventional type probes as the above mentioned C and D of which sensors are exposed, its fitting to the test specimen is identical as in the case of the previous test.

(3) Development of Fatigue Test

The development is as listed in Table 3-8.

(4) Results of AE Monitoring

a) At about 5000 cycles, a visible crack initiated. There was no much change seen in AE performance before and after the initiation of the crack. The AE count-rate rise prior to the rupture of the tube which occurred at 6897 cycles was observed to commence from around 6700 cycles.

Table 3-8. BR-4 Test Development

Time	Load	Frequency	Cycle Counts
Mar. 4	Ton	cpm	
14°10'	0 - 0.5	2	5.5
–	0 - 1.0	2	11
–	0 - 1.5	2	16.5
–	0 - 2.0	2	22
15°30'	0 - 2.0	8	540
2°25'	0 - 2.0	8	1,501 (Resumed after temporary suspension)
Mar. 5			
4°00'	0 - 2.0	5	4,234 (Resumed after temporary suspension)
–	0 - 2.0	2	4,500
8°40'	0 - 2.0	5	5,003 (Resumed after temporary suspension)
–	0 - 2.0	8	5,621
–	0 - 2.0	1	6,813
14°12'	0 - 2.0	5	6,897 (Ruptured)

But it was not as conspicuous in this BR test as in the case of the previous BE test.

b) This test was a load controlled test, and the tube rupture occurred at the upper part of the branch root. The AE detection (Probe A) at the upper part of the main pipe and

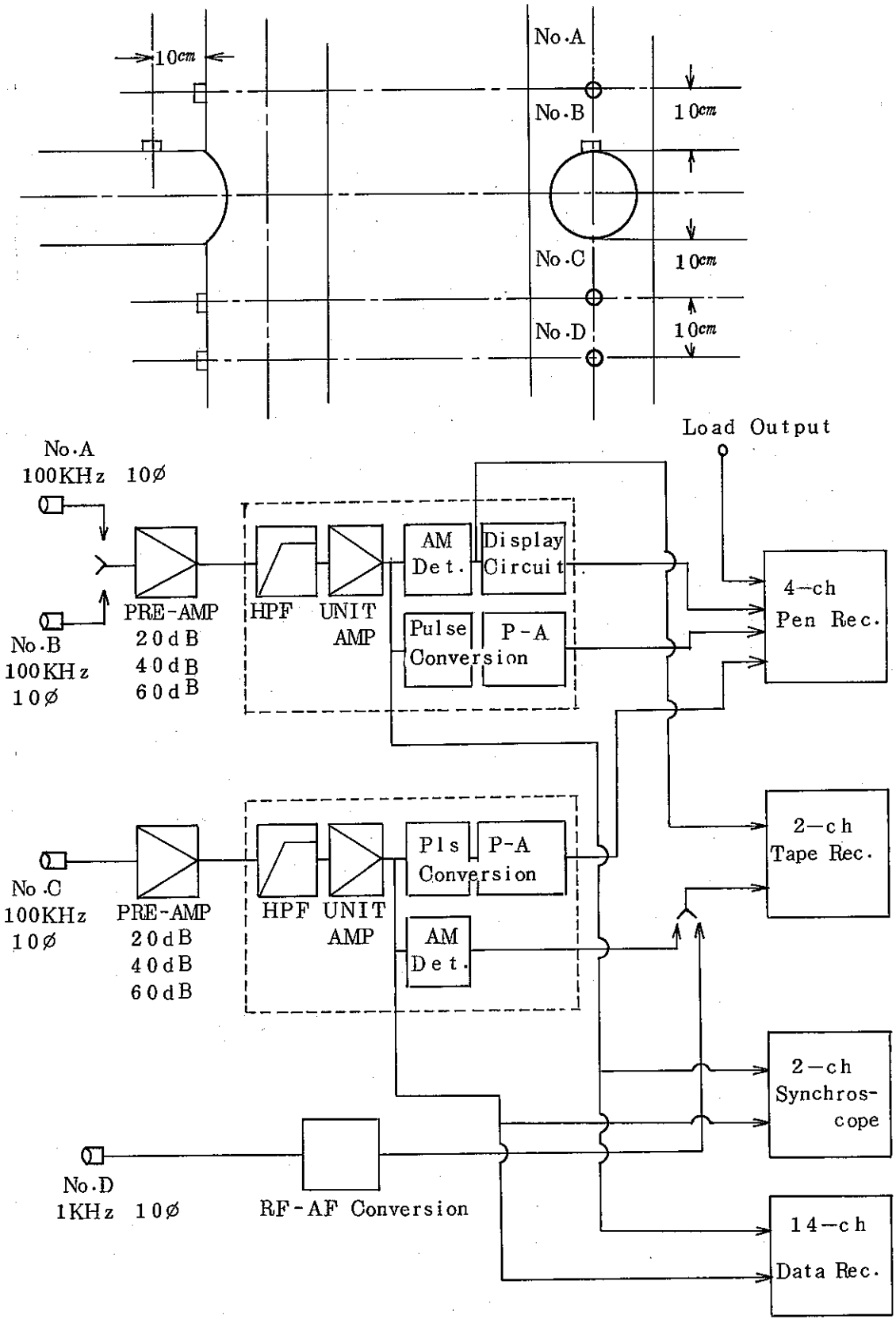

Fig. 3-9 Schematic Drawing of AE Monitoring in BR-4 Test

the AE detection (Probe C) at the lower part differed from each other. The latter had a lower counts of AE. From this, it was known that the distance between the signal emitting position and the sound probe position effectuated some influence on the AE detection.

c) The difference between the exposed and the closed type probes was at least very small in the frequency range of a 100KHz level. For the practical purpose, the closed type was found more desirable.

d) The 1MHz component of AE signal, as in the case of the AE of 600KHz component at the time of the BE test was rarely detected before crack initiation, while after the initiation of a crack, it showed comparatively a large amount of detection.

3-5 BR-5 Test

(1) Object of AE Monitoring

a) AE performance under the load controlled BR test. (fully reversed ±2ton load)

b) Effect of AE detection system improvement.

c) Preliminary test of AE detection method by means of high temperature probes and waveguides.

(2) AE Monitoring System

Fig. 3-10 represents the schematic drawing of AE monitoring system employed in this test. The sound probes of No. 1 and No. 2 in the drawing are heat-proof up to about 100 °C. No. 1 is fitted by way of a stainless steel rod of 18 mmϕ and 300mm long (one end is welded to the pipe and the other end is welded to the probe fitting plate.)

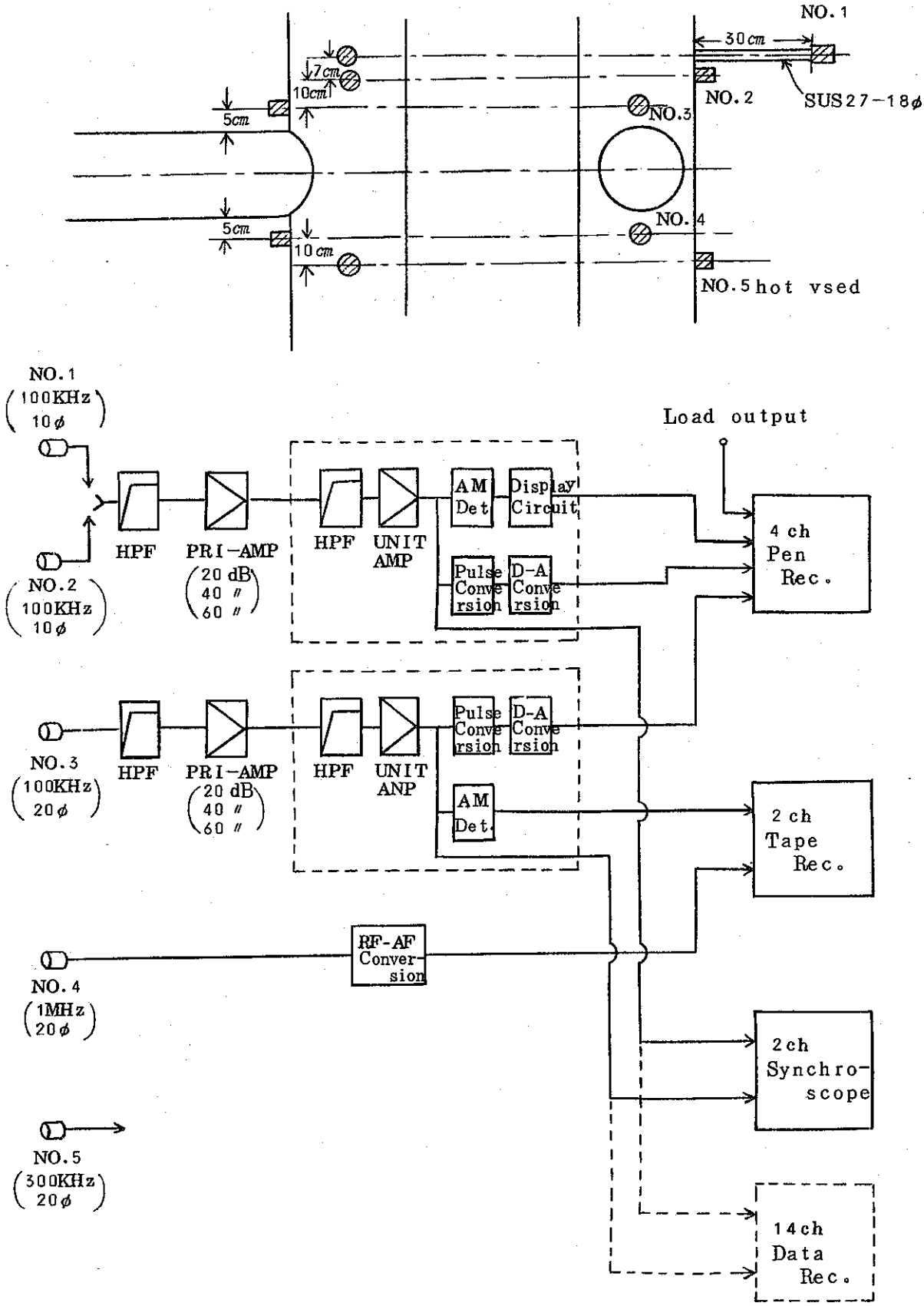

Fig. 3.10 Solematic Drawing of AE Monitoring in BR-5 Test

(3) Fatigue Test

The development of the fatigue test is as shown in Table 3-9.

(4) Results of AE Monitoring

a) In the previous BR-4 test, AE data before and after the detection of a visible crack showed no much difference. For this reason, the gain of the pre-amplifier was raised to the maximum of 60dB to heighten its sensitivity. In order to prevent the subsequent saturation of the pre-amplifier with the low frequency, large amplitude noises, a high pass filter was inserted in between the probe and the pre-amplifier, of which result, however, turned out to deteriorate S/N ratio and made it easy to pick up outer electrical noises.

b) The AE performance monitoring in this BR test was not satisfactory due to the above reason. But it could be said that the AE amplitude and its count-rate were both viewed small in comparison with those of the BE test.

c) For the sake of the high temperature test scheduled for the next time, two heat-proof probes were prepared and fitted at more or less the same location, one directly on the pipe, and the other through a waveguide. This way, the AE detection performance was compared in the monitor system. As the result, it was known that almost no attenuation of AE propagation by the waveguide was seen, and that the similar AE data could be obtained.

d) By inputting into the X-Y recorder the AE count-rate signal and the load signal, a study was made to find out at

Table 3-9 Development of BR-5 Test

Time	Load	Frequency	Cycle Counts
	Ton	cpm	
Apr. 12			
–	±0.7	1	1
–	±1.0	1	5
–	±1.5	1	8
–	±1.5	8	11
–	±1.75	1	52
–	±2.0	1	54
20°30'	±2.0	8	57
Apr. 13			
10°28'	±2.0	8	7,000
Apr. 14			
13°40'	±2.0	8	18,496 (Resumed after temporary suspension)
Apr. 15			
15°26'	±2.0	1	30,807
16°21'	±2.0	8	30,869
Apr. 16			
1°32'	±2.0	8	33,250 (Resumed after temporary suspension)
19°53'	±2.0	8	42,000 (Suspended for color check)
22°30'	±2.0	8	42,001 (Resumed)
Apr. 17			
8°57'	±2.0	8	47,000 (Temporary suspension)
10°30'	±2.0	8	47,003 (Resumed)
13°08'	±2.0	8	48,240 (Crack penetration)
–	±2.0	8	49,915 (Finished)

which phase of a load cycle AE would occur. As the result, it was recognized that the AE signal initiation was neither necessarily at the highest nor the lowest of the load, and that the AE count phase changed according to the cycle numbers.

3-6 Branch Tube, BR-6 Test (High Temperature Test)

(1) Object of AE Monitoring

a) To grasp AE performance features in the BR test at a high temperature of 550 °C.

b) To improve AE monitoring system.

(2) AE Monitoring System

The schematic drawing of the AE monitoring system in this test is as shown in Fig. 3-11. During this BR-6 test, in the third stage following 100,000 cycles, the display system of AE data was improved to display, besides the AE count-rate, the cumulative total of AE counts by a scaler.

(3) Fatigue Test Development

As this was a high temperature test, there were provided a heater and heat insulation materials around the pipe. In order to examine and confirm the cracks and their penetration, the test was suspended two times for a prolonged period at each time. In the first place, the temperature was restored to the room temperature, and the heater and the insulation material were removed. Because of this, this test was performed in three stages. Namely, the first stage was up to 10,000 cycles, and the second stage up to 100,000 cycles and the third one was above 100,000 cycles. The test development at each stage is given in Table 3-10.

Table 3-10 Development of BR-6 High Temperature Test

Time	Displacement (ton)	Temperature(°C)	Repetition Speed(cpm)	Cycle
1st Stage				
May 2, 9°50'	(-0.5 ~ 0.4)	550	1	1
–	(-0.8 ~ 0.5)	550	1	4
–	(-1.0~0.45)	550	5	9
10°32'	(-0.4 ~ 1.0) -4.0 ~ 5.0mm	550	5	146
May 3, 19°27	(-0.4 ~ 1.0) -4.0 ~ 5.0mm	550	5	10,000 (Heat off)
21°05'	(±0.5)	400	1 5	–
–	(±0.75)	400	1 5	–
May 4, 8°36'	(±1.0)	78	1 5	–
2nd Stage				
May 13, –	(±0.5)	RT	1	–
May 14, –	(±0.5)	130	1	–
–	(±0.5)	300	1	–
–	(±0.5)	400	1	–
–	(±0.5)	500	1	–
May 18, –	-4.0 ~ 5.0mm	550	2	10,001
–	-4.0 ~ 5.0mm	550	5	10,250
May 20, 14°00'	-4.0 ~ 5.0mm	550	8	24,030
21°30'	-4.0 ~ 5.0mm	550	10	28,000
May 25, 22°25'	-4.0 ~ 5.0mm	550	10	100,000 (Heater off)
–	–	RT	–	–
3rd Stage				
Sept.27, –	–	RT	–	– (Temp. raised)
Sept.28, 17°13'	±7.5mm	550	8	100,001
Oct.2, 5°54'	±7.5mm	550	8	140,000 (Finished)

(4) Results of AE Monitoring

a) As this was the first high temperature test of the AE measurement, the primary object of this AE monitoring was to check on the high temperature AE performance characteristics. The test was performed in three stages of up to 10,000 cycles, up to 100,000 cycles, and above 100,000 cycles where the crack initiation took place. In each of these three stages, the AE monitoring detected several new facts. Namely, in the first stage, signals of large amplitude were detected frequently, and they posed a big problem as it was difficult to determine whether they were AE signals or some other noises. Then, in the second stage, AE signal amplitude and AE count-rate rose along with the rise of temperature, and it was also noticed that the AE count-rate changed in proportion to the variation of the maximum and minimum of the bending load values. In the last stage, it was known that the display of AE cumulative total counts by means of a scaler which was incorporated into the AE monitoring system concurred well with the development behavior of the fatigue crack.

b) As shown in Fig. 3-12, stainless steel piping element emits few acoustic signals in room temperature, but both signal amplitude and emission rate increase when the temperature is elevated.

c) As shown in Fig. 3-13, in the third stage where the amplitude of the controlled displacement was incremented, the AE cumulative total counts showed a straight linear change of a certain gradient when there was no material property

change such as an initiation of a crack. Upon an initiation of a crack and in the process of its development, this linear gradient showed some changes which strikingly increased as approaching closer to rupture. Then relation between the AE amplitude and the count-rate was different before and after the initiation of a fatigue crack. That is, the logarisms of the above two are, as shown by Fig. 3-13 b), in a negative gradient straight line relation, and this gradient showed different values before and after the initiation of a fatigue crack. After the initiation of a crack, the AE amplitude and counts gradually grew fulfilling this relationship.

d) From the outcome shown in Table 3-11, the signals which were detected by the sound probe of 100KHz resonance were considered not noises but AE signals produced following the plastic deformation of the piping material itself.

e) For the AE monitoring system of this test, a new pre-amplifier was prepared and in addition a lowpass filter for the 50Hz AC power source was applied as a countermeasure to the decline of S/N ratio, i.e., for elimination of noises which were the problems of the previous BR-5 test. As the result, it was possible to eliminate almost completely the electrical noises emitted from cutting, welding, crane operation, etc. in the measuring environment.

However, raising the input impedance by way of adding a 1ER20 vacuum valve in the pri-amplifier to detect AE with high S/N. However, due to the large amplitude and high count-rate of AE signals under a high temperature, the pri-

amplifier had to be removed during the third stage (at about 100,100 cycles) and its use was temporarily suspended.

Table 3-11 AE Performance Under High Temperature BR-6 Test

AE Signal Performance	AE	Noise from non-operating system	Noise from jack operation	Noise from heater
(1) Branch pipe's bending displacement cycle and AE signal synchronize	O	X		
(2) AE ceases as jack operation stops	O	X		
(3) Changes in AE count-rate peak synchronizes with the variation of the max. load value	O	X		X
(4) Counts due to heater stop are very few	O			X
(5) AE counts rise when displacement stroke gets larger	O	X		
(6) No visible Kaiser effect is noticed	O			
(7) AE counts at the max. side and the min. side of displacement differ from each other	O	X		
(8) AE is not frequent in bending load cycle when temperature declines	O	X		
(9) AE is extremely seldom at the load cycle under room temperature as the previous tests	O	X	X	
(10) AE rises at the load cycle under a rising temperature	O	X	X	
(11) AE volume drastically rises as approaching closer to rupture	O	X	X	X
Note: O; Possible,		X; Not possible		

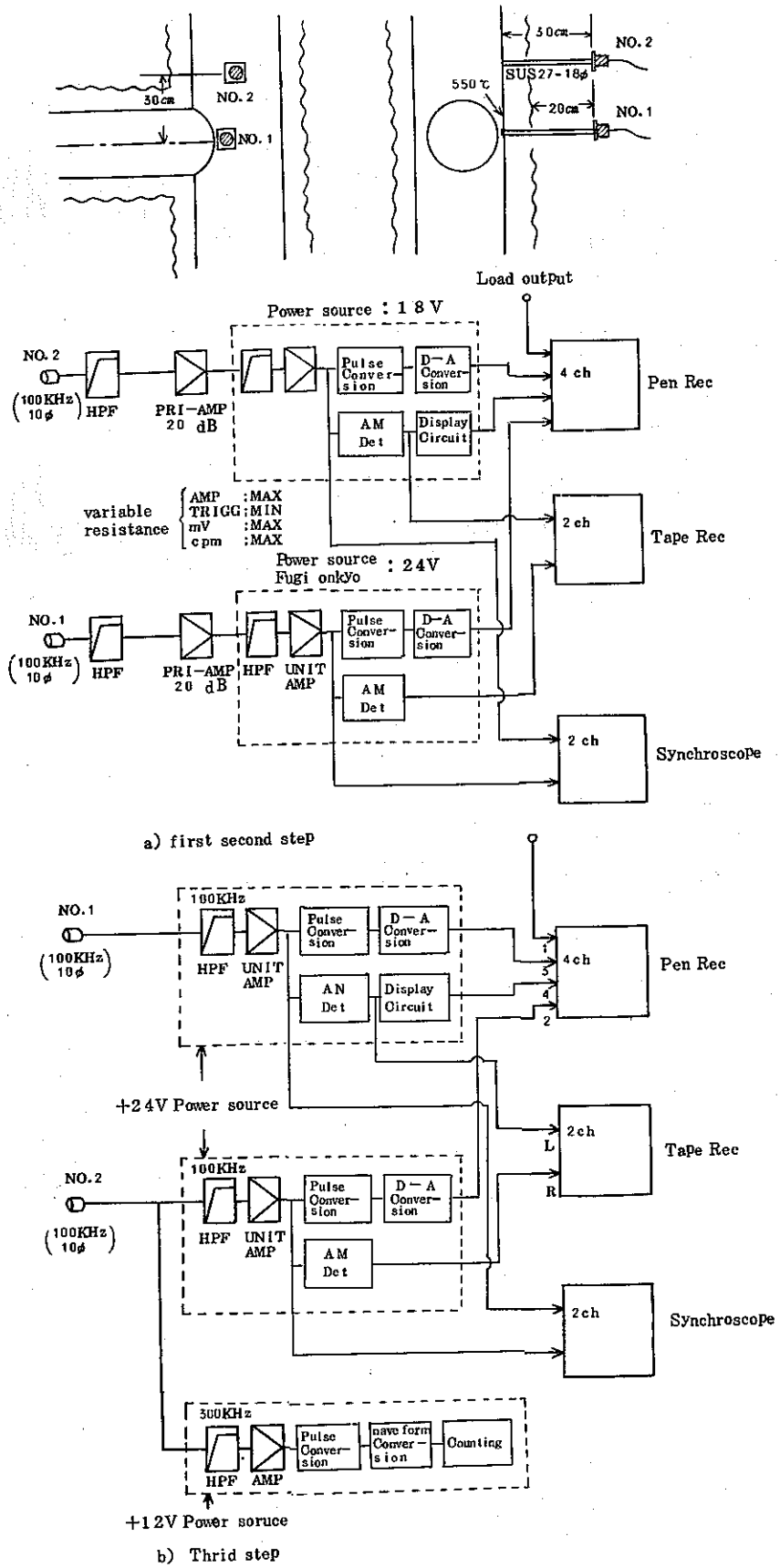

Fig. 3-11 Schematic Drawing of AE Measuring System in BR-6 High Temperature Test

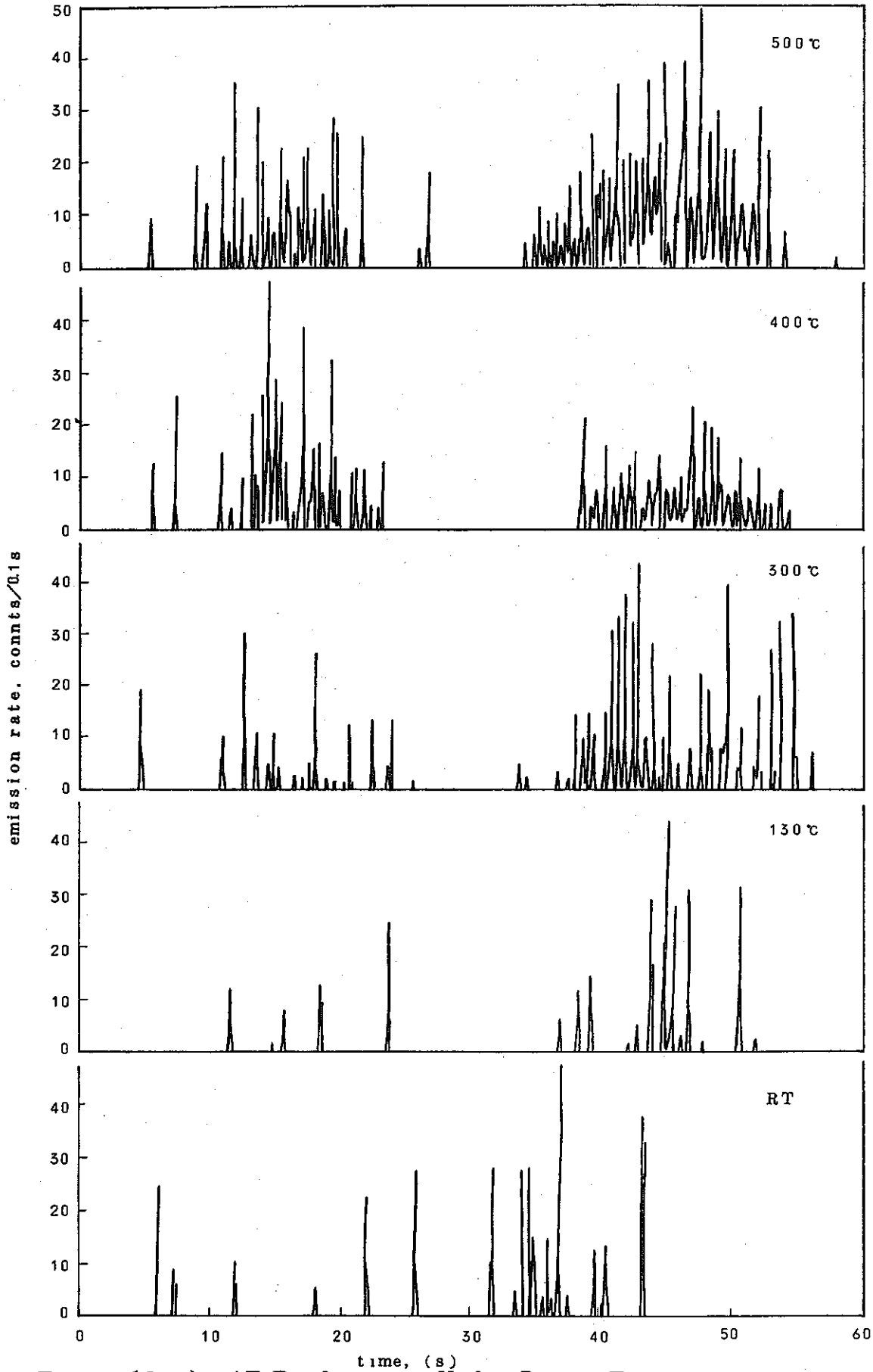

Fig. 3-12 a) AE Performance Under Rising Temperature in BR-6 High Temperature Test (1)

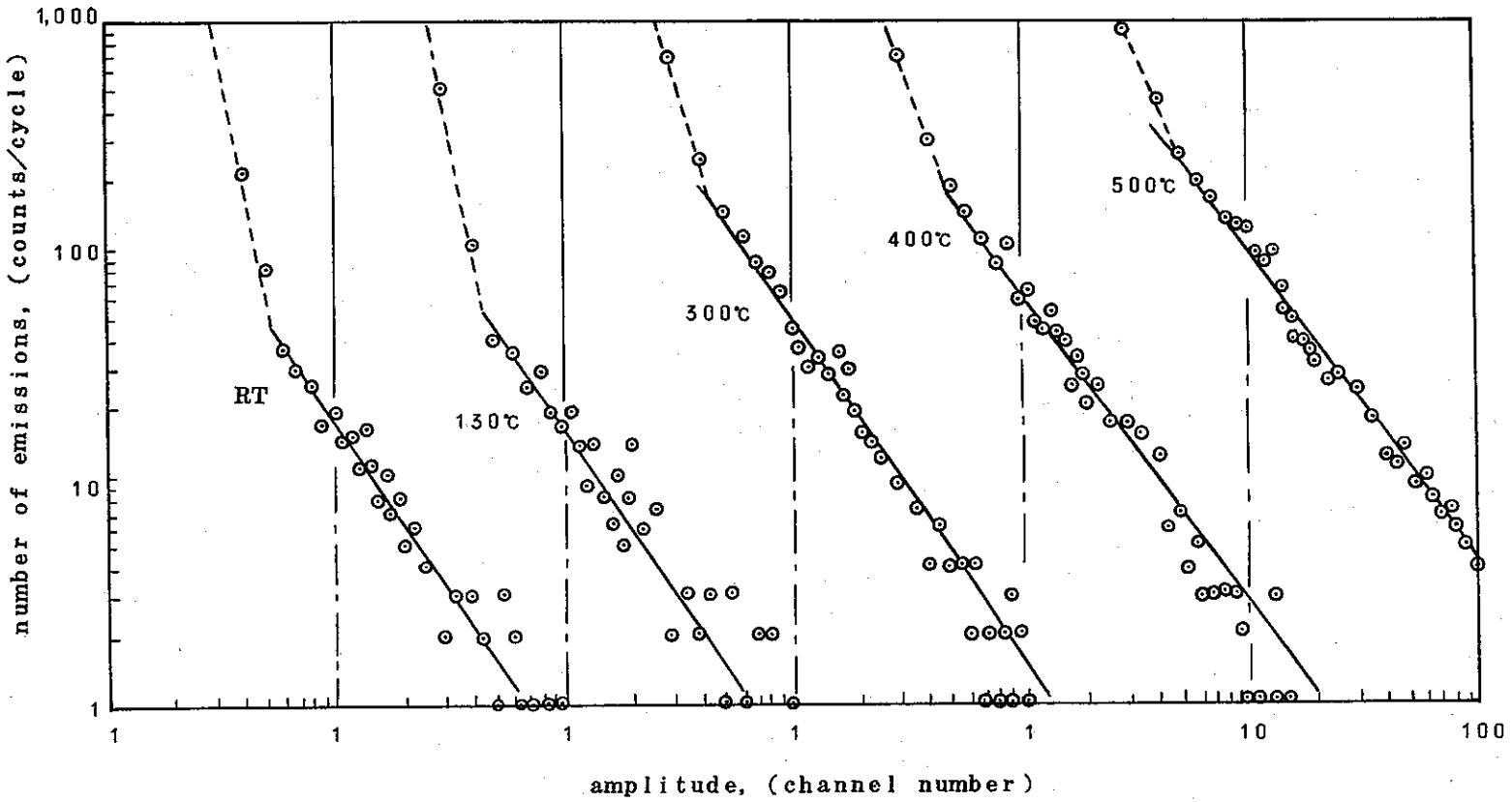

Fig. 3-12 b) AE Performance Under Rising Temperature
in BR-6 High Temperature Test (2)

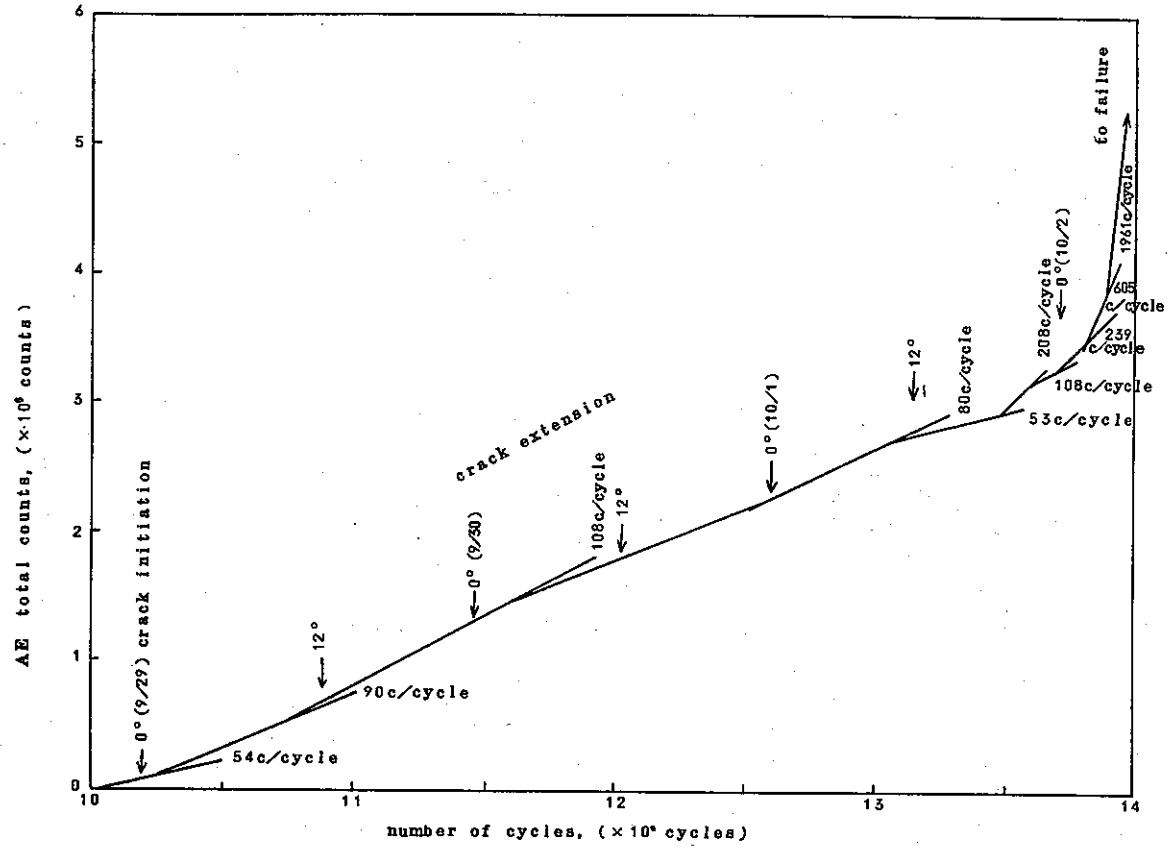

Fig. 3-13 a) Time Change of AE Cumulative Total Counts in BR-6 High Temperature Test

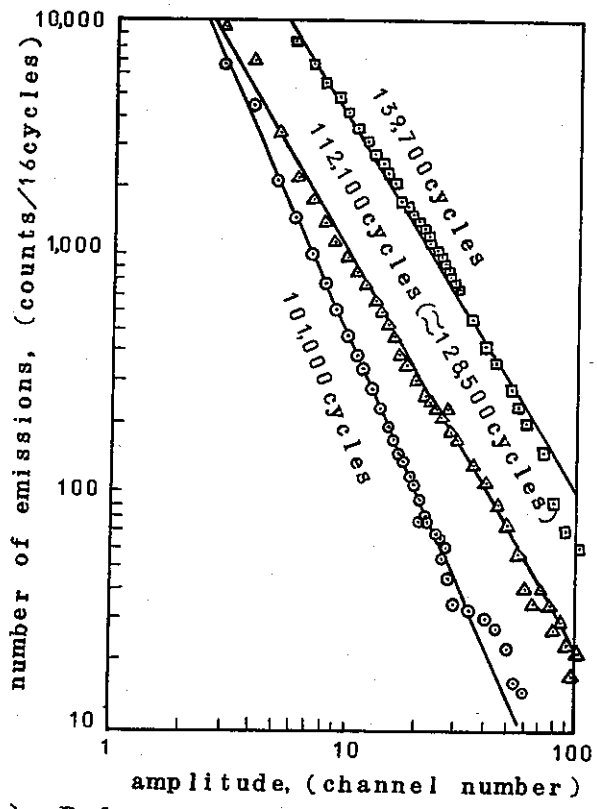

Fig. 3-13 b) Relation Between AE Count Rate and Amplitude in BR-6 High Temperature Test

4. Assessment and Review

4-1 AE Detection Technique

(1) Preparation of AE Monitoring System for Fatigue Test of Piping Components

The AE detection in the five fatigue tests of piping components from the first BE-4 test to the final BR-6 test were mainly aimed at building up AE detection and monitoring system and its improvement.

In the first BE-4 test, the AE measuring system No. 1 developed by CRIEPI for small test pieces, was applied to the piping structure, and the resulting outcome was more or less satisfactory. The improved AM radio set for measuring 600KHz AE was found in the course of the test to have some problems of picking up electrical noises and requiring a higher detection sensitivity. Since measurement of AE signals with such high frequency as 60KHz or 1MHz contains several problems involving structure of the sound probes, the frequency performance of the pre-main amplifier, frequency filter circuits, etc., the task of building-up and improvement of the system has not made sufficient progress up to the time of the BR-6 test. This was also partly due to the fact that our work was mainly concentrated to the measuring system of 100KHz signal of AE during this period.

The 100KHz AE measuring system was capable of monitoring the AE count-rate alone in the BE-4 test, and there was available only one unit of this system. In the BE-5 test, an additional measuring system was provided so that both AE count-rate and AE amplitude could be monitored. But since

this new system was for a preliminary study for manufacturing a practical measuring system to use in a future atomic power plant, it was not employed in the subsequent BR tests.

For the BR-4 test, a new measuring system No. 2 was manufactured having more or less the same circuit composition as that of the 100KHz measuring system which was used in the BE-4 test. This new system was capable of monitoring not only the AE count-rate but also the time change of AE amplitude. But in the tests of BR-4 and BR-5, there arose a problem of mutual interference when these two units were operated with the same DC power source. Particularly, in the case of BR-5 test, possibly due to the problem of S/N ratio decline resulting from the high pass filter placed next to the sound probe in order to raise the sensitivity of the pre-amplifier, the AE monitored data were affected by noises of various sources which greatly disturbed the AE occurrence with the fatigue crack. Thus, it was difficult to obtain an appropriate AE monitoring corresponding correctly to the fatigue crack.

For this reason, for the BR-6 Test, a vacuum tube installed pre-amplifier with a high input impedance was made, and a new high frequency AE measuring system No. 3 with a scaler incorporated in it was also made. This system was provided with the frequency filter circuits of 300KHz, 600 KHz and 1MHz respectively, and was capable of displaying the monitored AE count-rate. This unit was employed in the 3rd stage of the BR-6 test and proved very effective. Particularly, the monitoring of AE cumulative total counts was

effective in grasping of the whole process involving crack initiation - progress - penetration.

In the BR-6 test, cumulative number of AE was monitored simply by reading periodically the figure displayed on the counter, when the AE count rapidly increased at the final stage of the test, there arose a problem of shortage in the number of display tubes. For this, a study is now being made to add more number of display tubes and the cumulative tot al counts can be displayed on a chart recorder.

Fig. 4-1 shows the circuit arrangement in the measuring system No. 1 which was employed in BE-4 test. Fig. 4-2 represents the circuit arrangement drawing of the measuring system No. 2 which was applied to BR-4 test and after, and Fig. 4-3 gives the circuit arrangement drawing of the measuring system No. 3 used in BR-6 test.

(2) Structure of Sound Probe and Its Fitting Method

The structure of the typical model of sound probes used during the tests is as shown in Fig. 4-4. In the BE-4 test and early stage of BR tests, the exposed type probes shown by Fig. 4-4 b) were employed. But as this type of probes was bound to the pipe by a metal band, it presented a structural weakness. In the latter stage of the test, the closed type probes shown in Fig. 4-4 a) were employed. This model is a heat-proof type capable of withstanding 100 $^{\circ}$C or more.

A closed type probe is strong in its construction, but has a weakness of declining its resonant frequency. Consequently, although the frequency of 100KHz range suffers little

trouble of this effect, for a high frequency AE probe of 1MHz range, an exposed type is desirable. At present, it is planned to make probes of various structures including the exposed type for the purpose of investigating their frequency or sensitivity performances.

For the fitting of a sound probe, a small band was used to bind the probe directly to the pipe. In the tests of BR-5 and BR-6, as the waveguide type gave a good result, this method was considered desirable for the future tests. The fitting method of this type of sound probes is to weld one end of the waveguide to the pipe and the other end to a metal plate to which the sound probe is fixed by a screw nut. In between the metal plate and the probe, a piece of paper coated with silicon-grease is applied as an electrical insulation. A solid rod of either stainless steel or soft steel of 6mmϕ and 18mmϕ and 20 - 30cm long were used as a waveguide. The material property and the diameter affected to some degree the detection sensitivity, but such small effect was considered to be sufficiently offset by an increase of gains in the pre-amplifier connected to the sound probe and the main amplifier.

The question of the appropriate location of the sound probes was studied several times during the tests. In some cases we obtain a conclusion that a distance of a few meters from signal emission point affected but little on AE signal detection, while in other cases we observed a marked difference in AE signals from two probes located respectively 10cm upward and downward from the joint-section of a tee. It is, therefore, considered that further elaboration on this subject

may be necessary in the future tests. As these problems also relate with the position estimation of AE, new measuring systems will be required for a quantitative evaluation.

As a preliminary study of the fitting of the waveguide for the high temperature (550 °C) test, an approximate calculation of the temperature distribution in the waveguide was performed as follows: In this case the waveguide is hypothetically set as natural-cooled and of infinite length. With the arrangement as shown in Fig. 4-5, the following equations can be obtained:

Heat flow conservation: $qx = q_x + dx + q_g$

Heat transfer: $q_g = \alpha \cdot nd(T - T_o)\,dx$

Heat conduction: $q_x = -\lambda S \frac{dT}{dx}$

" " : $q_x + dx = -\lambda S \frac{d}{dx}\left(T + \frac{dT}{dx}\,dx\right)$

where, d : Rod diameter

α : Heat transfer coefficient

$S = \frac{n}{4}d^2$: Rod cross section

λ : Heat conductivity

Fig. 4-5 Temperature Gradient Calculation of Waveguide

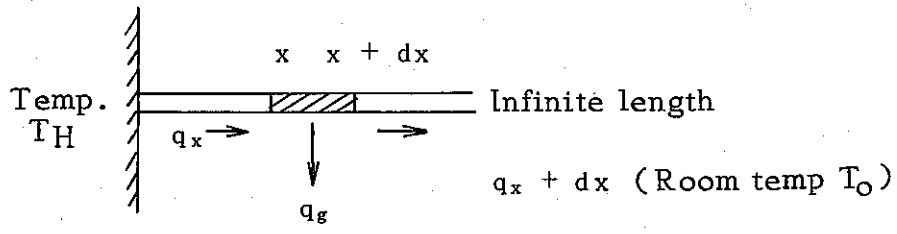

From above equations, the following equation can be obtained:

$$\frac{d^2T}{dx^2} - K^2 (T - T_o) = 0$$

$$K^2 = \frac{n d a}{\lambda S} = 4d/\lambda d$$

The boundary conditions are that $T = T_H$ at $x = 0$ and $T = To$ at $x = \infty$, from which $T = T_o + (T_H - T_o)e^{-Kx}$ is obtained as the equation for temperature distribution. For natural convection, α is given as follows:

$$\alpha = 1.14 (\triangle t/d)^{1/4} \text{ Kcal/m.hr.}^\circ\text{C}$$

$$\triangle t \fallingdotseq \frac{T_H - T_o}{2}$$

Replacing d = 0.018m, T_H = 550 °C, T_o = 20 °C, = 14 Kcal/m.hr.°C we obtain T = 84 °C at X = 0.15m.

As there were several hypotheses involved in the above calculation, the computation was made on a safety side, and actually, the probe's temperature was no higher than about 40 °C.

(3) AE Detection Method of High Sensitivity and S/N Ratio

AE has two types, one is the burst type of large amplitude and the other is the continuous type of small amplitude.

Following the initiation of a crack on the piping components, there occur large amplitude AE counts which are preceded and followed by small amplitude AE counts. The continuous type AE which had more counts was the measuring target rather than the burst type AE which had less counts. This required a highly sensitive AE detector. Though

detectors with high sensitivity are often prone to pick up noises, AE detectors should have high sensitivity and a high S/N ratio at the same time.

Elimination of electrical noises in the present tests was possible by means of a 50Hz low pass filter when the noises were from the AE power source, and when they were originated from the probe, the probe was insulated to make it floating. As for a stronger electrical noise environment, there is a prospect of solving it by application of a differential probe and a pre-amplifier. On the other hand, against the acoustic noise, so far it was possible to eliminate low frequency noises by way of a frequency discrimination, namely, by use of a high pass filter. But for the future, it is considered that application of a coincidence or an anti-coincidence methods would become necessary against a strong acoustic noise environment.

The noise level of the AE measuring system is generally determined in the pre-amplifier. For the coupling with a PZT oscillator, it was desirable that the input impedance of the pre-amplifier should have as high a value as possible. For this reason, a new model of vacuum tube type pre-amplifier with a high input impedance at a low noise level was made for the test. The circuit arrangement drawing of this model of pre-amplifier is as shown in Fig. 4-6. This model was employed in the 3rd stage of the BR-6 test. But due to the occurrence of a large volume of AE counts of large amplitude, its effectiveness will have to be judged according to the results of the future tests.

(4) Method of Recording and Analysis of AE Data

a) Amplitude.

b) Count rate or the cumulative total counts (time integral of the count rate).

c) Wave form or the frequency composition (Fourier transform of the wave form).

It is necessary that these three items should be studied and analyzed to determine their mutual relationship or inter-relationship as well as their relation with time, or displacement cycle. For the AE analysis in the present tests only the count rate - time and the count rate - amplitude relationships were analyzed on the basis of the tape-recorded data. But in the future, it will be necessary to analyze the load phase, wave form and frequency composition of AE signals.

For the analysis of frequency composition in the future, more effective use of high speed data recorders and transient recorders, and introduction of sound probes of broader band range will become necessary.

During the period of the present tests, the data analysis was performed based on the tape recorded data of audible range obtained through amplitude modulation of original AE signals. In this case, the tape recording was made either intermittently in each test or continuously during the whole test period. At present, it is considered more desirable that these data should have been recorded at certain set intervals as well as at times for 2 - 3 minutes when some changes occurred in the AE performance.

4-2 AE Characteristics of Piping

(1) Process of Fatigue Failure and Its Correspondence with AE Performance

It was recognized that the AE performance in the process of a fatigue failure of a piping component so far experimented (BE-4 upto BR-6) resembled fairly well to the process of the fatigue failure experimented with the small size tensile test pieces. That is:

a) At the initial cycle stage, there was observed a considerable amount of AE counts which were thought to be derived from a plastic deformation. Then the count rate decreased later on.

b) Upon the initiation of a crack, the AE count rate increased, and also the AE amplitude increased. The relation between AE amplitude and count rate, when expressed in logarism, is on a straight linear relationship with a negative gradient, and with the initiation of a crack, this gradient changes. That is, prior to the initiation of the crack, the gradient is comparatively large, of which value is generally constant. However, after the initiation of the crack, the gradient value declines comparatively smaller and maintains a constant value. In other words, the small frequency AE declines and the large frequency AE increases.

c) Approaching to a crack penetration or to a final rupture, AE count rate very rapidly rises. Although in the case of the small size tensile test pieces, the drastic increase takes place for a short time, in the case of the test of piping components, this time lasts relatively long, allowing a sufficient

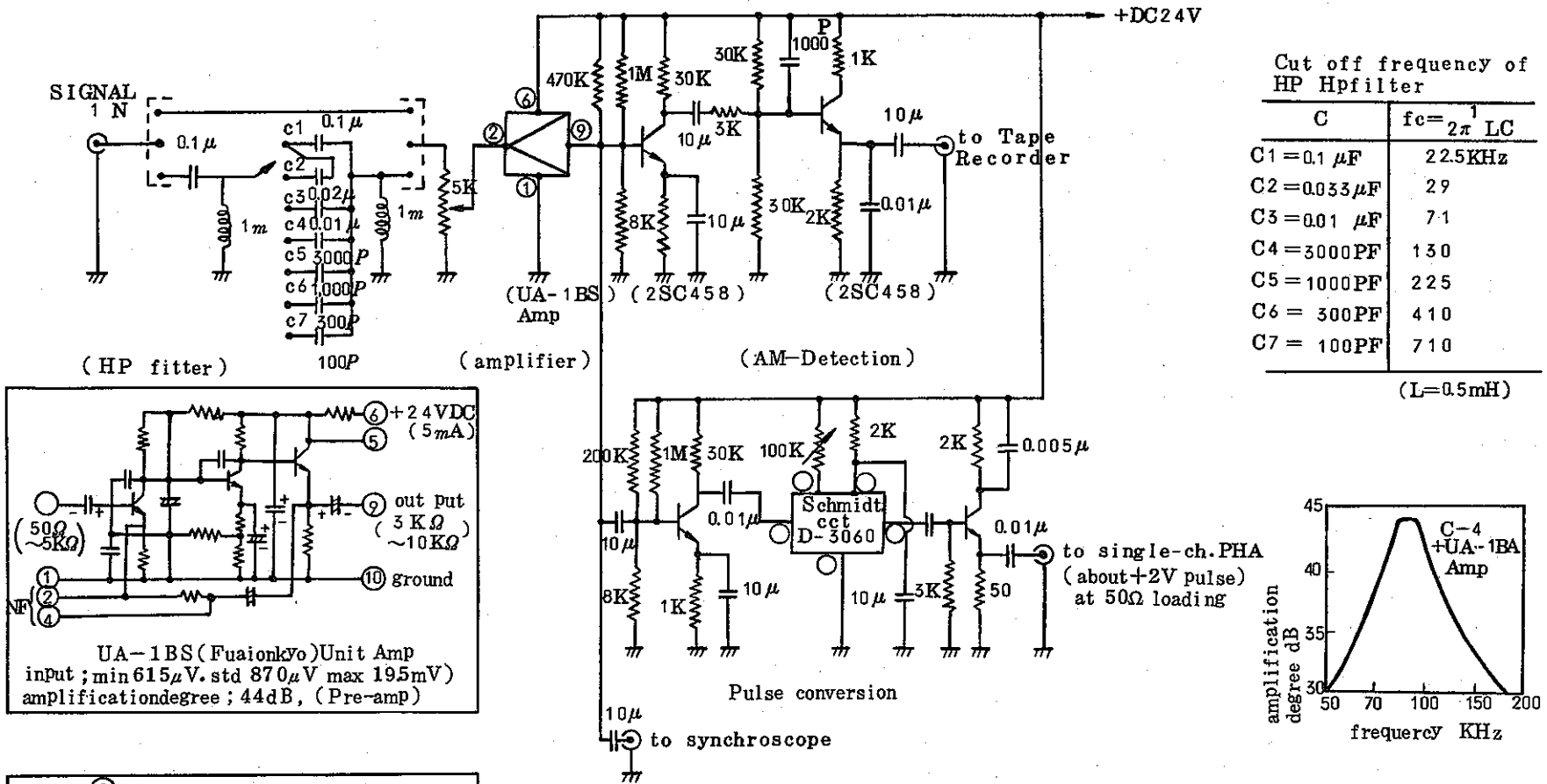

Cut off frequency of HP Hpfilter

C	$fc=\frac{1}{2\pi}\sqrt{LC}$
C1 = 0.1 μF	22.5KHz
C2 = 0.033μF	29
C3 = 0.01 μF	71
C4 = 3000PF	130
C5 = 1000PF	225
C6 = 300PF	410
C7 = 100PF	710

(L=0.5mH)

Fig. 4-1 Circuit Arrangement in AE Measuring System No. 1

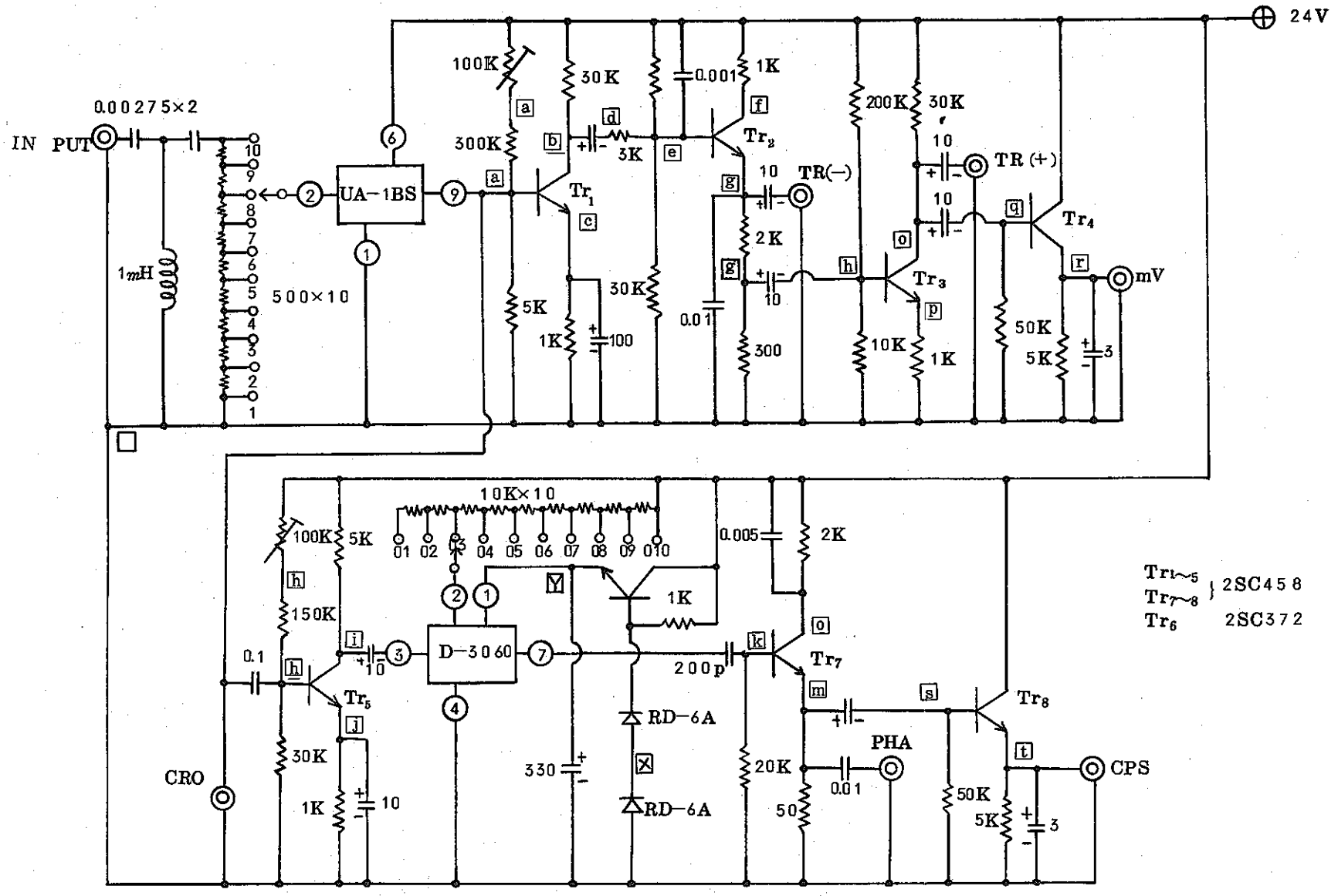

Fig. 4-2 Circuit Arrangement in AE Measuring System No. 2

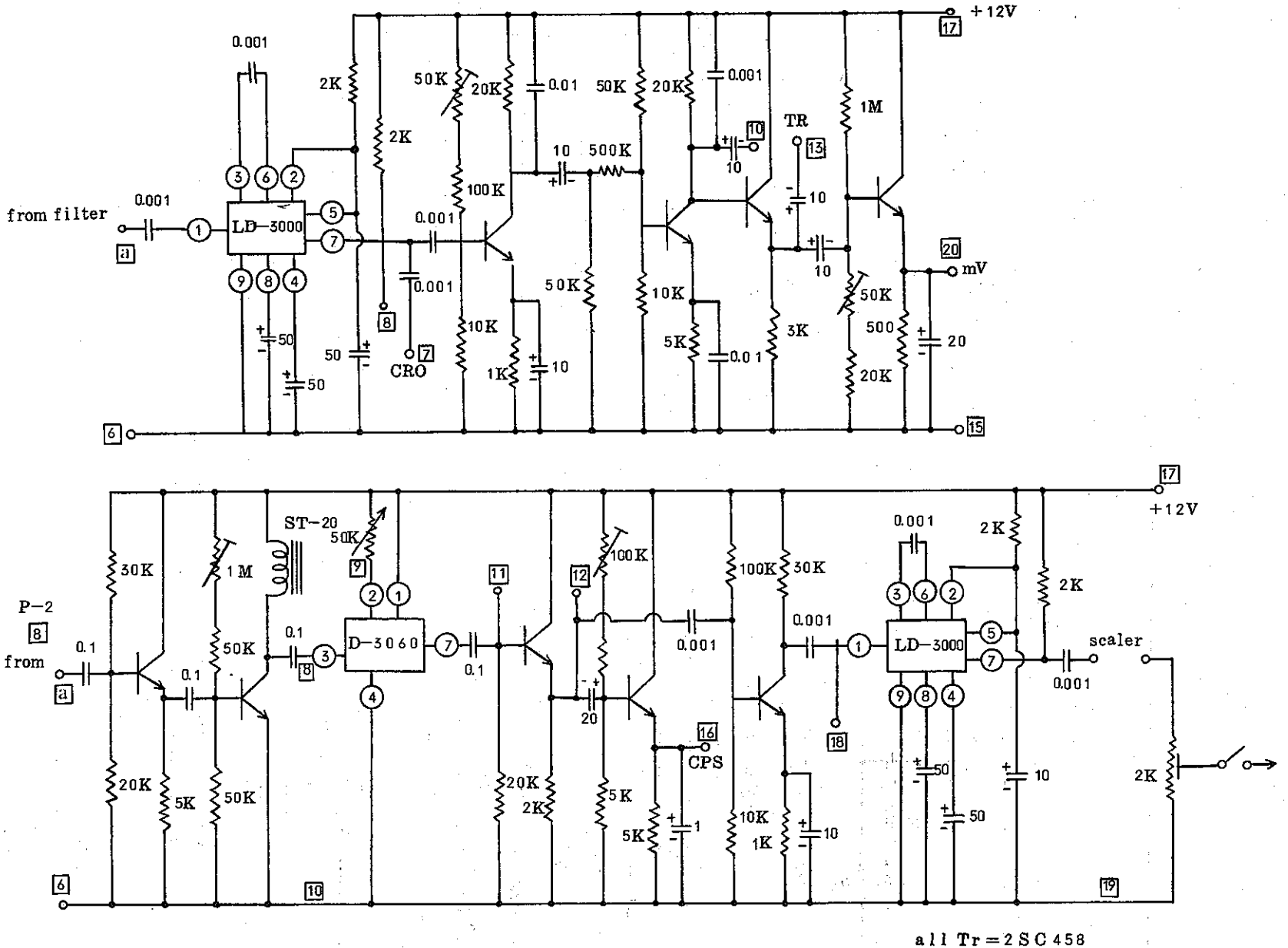

Fig. 4-3 Circuit Arrangement in AE Measuring System No. 3

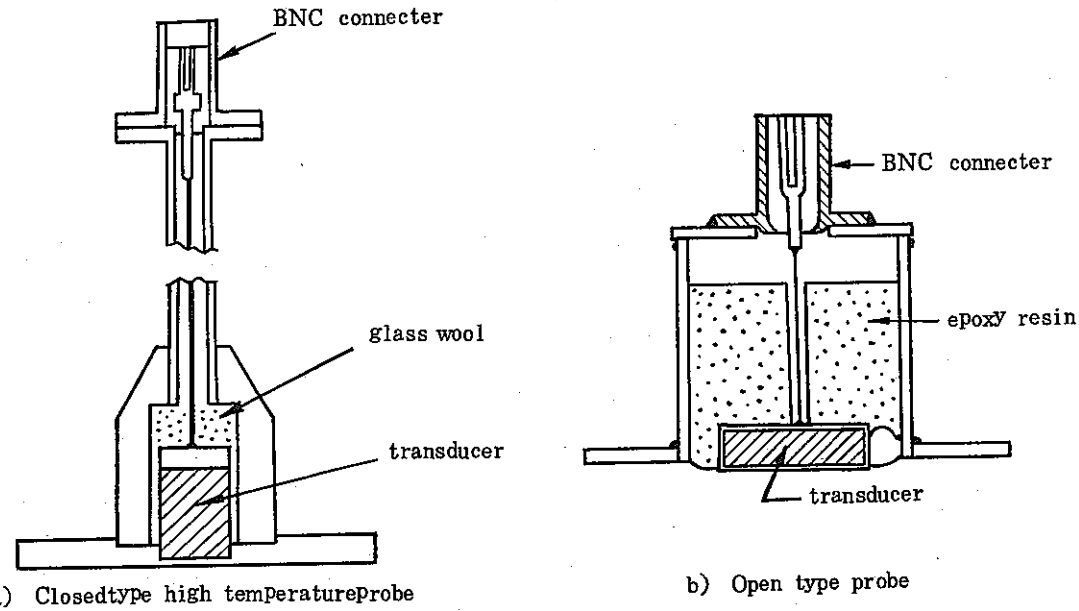

a) Closedtype high temperatureprobe

b) Open type probe

Fig. 4-4 Structure of acoustic probe

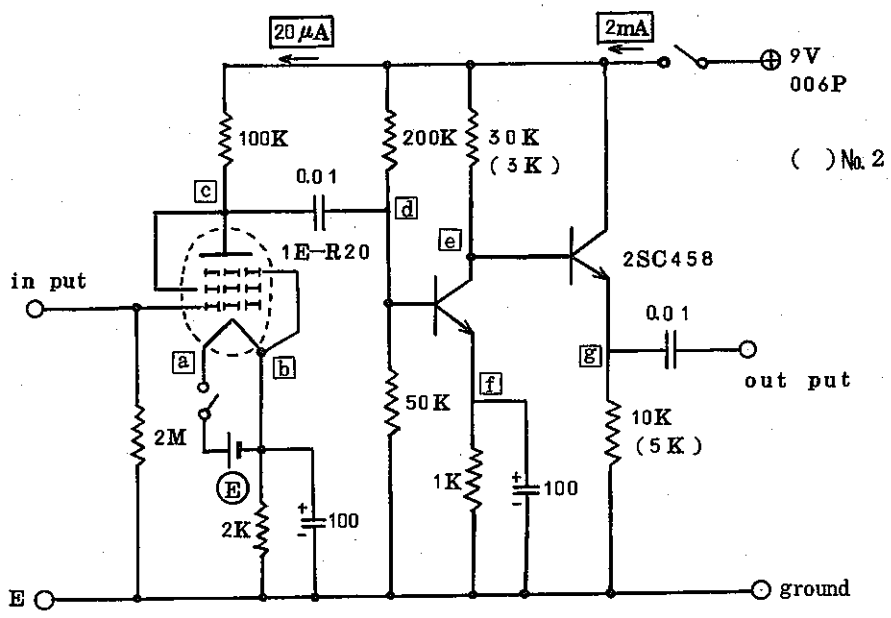

Ⓔ ; Furukawa, Ni-Cd Battery 125V

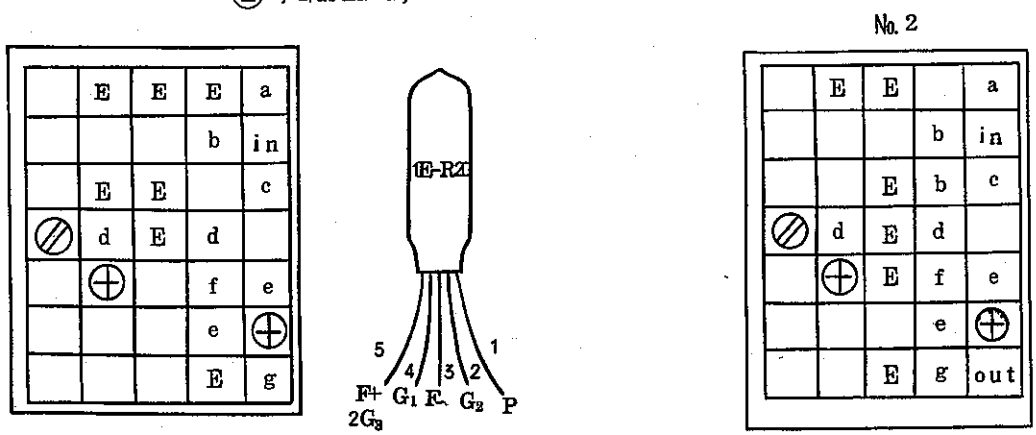

Fig. 4-5 Circuit Arrangement in Low Noise Pri-Amplifier of High Impedance

time to foresee the rupture.

These performance characteristics were reproduced under various conditions. They were observed both in bend and branch tube tests and under controlled load and controlled displacement and under room temperature and elevated temperatures. It is considered that the quantitative evaluation of AE performance observed in the tests under varied conditions should be undertake after a sufficient comparison has been made with those fatigue failure data measured with strain-gauges.

(2) AE Performance in High Temperature Test

As described in Section 3-6 "High Temperature Test of BE-6", it has been made clear that the 100KHz component of AE has a conspicuous temperature dependency. That is, when the temperature rises, both the AE count rate and amplitude rise. While in the room temperature test of the small size stainless steel test pieces, AE detection was extremely difficult, it was, by contrast, easy in the test under a high temperature close to the actual operation condition of the piping components, which was an interesting finding.

The reason is considered to be that since AE of 100KHz element was originated in a plastic deformation, such a plastic deformation became active as temperature rose higher.

Such AE characteristics are considered highly helpful in the application of the AE monitoring on the actually operating structures such as loops of the experimental FBR. This, along with the fact that the AE detection technique by way of a waveguide employed successfully in the high temperature

test is considered effectively applicable also to a high radiation environment is a significant finding for effectiveness evaluation of the AE technique.

(3) Discrimination of AE from Environmental Noises

In the process of the experiment from BE-4 to BR-6, there occurred on several occasions problems of environmental noises. In other words, in the state where the bending cycle movement stopped, any acoustic noise of over several 10KHz frequency range could well be ignored, and even at the fatigue cycle, as the AE count rate fell to a minimal level, it is thought any acoustic noises caused by jack operation, etc., could be almost completely eliminated by a high pass filter. But it can be said that, in most cases, discrimination of AE from the environmental acoustic noises was successful thanks to the use of frequency filtering circuits.

In the future, if an application of the coincidence AE detection or the anti-coincidence AE detection by use of a main acoustic probe and several auxiliary probes could be worked out in relation with the position-determination technique for AE, the discrimination of AE from the environmental noises would be further improved and become much easier.

(4) Utilization of AE Data at Initiation of Fatigue Test (Preliminary Cycle.)

Prior to the initiation of the fatigue test, low amplitude repetition tests of load or displacement of several cycles are being performed. These repetition tests have the same effect as that of the hydrostatic test in the pre-service inspection, and it is expected that data on the soundness of the

piping material, presence of defects, etc., will be obtained.

At present, the data of the five tests of BE and BR have been obtained. Within the extent of these results, it has been confirmed that AE counts were higher with those tubes which had relatively quick crack penetration, while AE counts were low with those tubes which took relatively a longer time for crack penetration. But these data are not yet sufficient, and has not yet reached a stage where the relation of AE data with the difference between the forecast and the actually measured value of the crack-penetration cycles can be quantitatively grasped. These are left as the subject of future research and study.

5. Conclusion

This is an interim report of the experimental research on "Follow-up Method of Fatigue Failure Process on FBR Primary Sodium Coolant Piping Loop by Means of Acoustic Emission Monitoring" which is undertaken jointly by PNC and CRIEPI, and contains the information on AE detection technique and data obtained in a series of AE monitoring of fatigue failure of piping components involving five tests beginning with the room temperature test of BE-4 in February, 1972, up to high temperature test of BR-6 in October, 1972. It also contains some data of AE monitoring of small size stainless steel test piece fatigue tests.

Although this report covers a short period of time, several interesting findings relating to the application of AE technique have been brought to light such as the possibility of monitoring fatigue failure of stainless steel piping components, AE high temperature performance, etc., and various new developments have been achieved on AE technique itself.

The future experimental and development work is scheduled to be undertaken along with the programs shown in Table 5-1 in concert with the program of the piping structure fatigue tests to be undertaken by PNC.

Table 5-1 Future Research Plan and Time Schedule

Research Items	1972 Oct-Dec	1973 Jan-Jun	1974 Jul-Dec
(AE Technique)			
(1) Optimum structure of a sound probe	O		
(2) Optimization of acoustic coupling to the testing subject	O	O	
(3) Development and application of AE detection system for double tubes	O		
(4) Establishment of AE detection system under high temperature, high radiation environment	O	O	
(5) Realignment of AE performance direct monitoring system and its data recording system	O		
(6) Multi-stage and multi-channel of AE monitoring system		O	
(7) S/N ratio improvement and positional determination by means of the coincidence method		O	
(8) Evaluation of the optimum monitoring system		O	O
(AE Performance)			
(1) Analysis of AE amplitude and AE count rate	O	O	O
(2) Analysis of AE wave forms and frequency		O	
(3) Grasping of the performance of AE signal and the environmental noises		O	
(4) Grasping of the correlation between the fatigue failure process and AE performance	O	O	O
(Review and Evaluation of Effectiveness of AE Technique)			
(1) Review on the absolute calibration method of AE monitoring sensitivity		O	O
(2) Review on the long-term stable performance reliability of AE monitoring system		O	O
(3) Evaluation of the effectiveness and usefulness of AE technique			O

Referential Literature

Translation omitted.